CHAPTER – 1

Introduction

History of Perovskite

Perovskite having the general formula ABO_3 known as simple Perovskite oxide. The Perovskite oxide was first time discovered by Gustav Rose in 1839 in the Urai Mountain of Russia. The term Perovskite was taken by the name of Russian Mineralogist L.A. Perovskite (1792-1856). Perovskite having the chemical formula ABO_3 where A exists at the corner at the cubic lattice, B exists at the body-centered, and oxygen occupied at the face of the cubic lattice. In the perovskite system the size A always greater than that of B. (Abe and Uchino 1974). The structure of the Perovskite is shown in Figure 1.1. It is observed that B represents mainly 3d, 4d, and 5d transition metals. The metal is occupied by an octahedral position BO_6 and surrounded by oxide ions. (Fang et al. 2012 p. 15) In Perovskite system A represents the Alkaline earth metals. (Lawn et al. 2016),(De Almeida-Didry et al. 2018), (Tripathy et al. 2016) ,(Dion et al. 1981), (Domen et al. 1990)

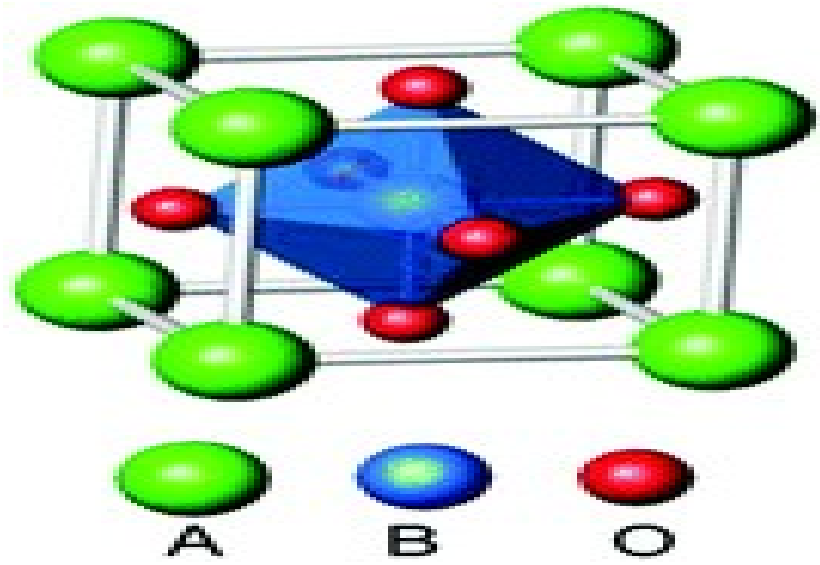

Figure 1.1 shows the Perovskite structure (Rabuffetti and Brutchey 2014)

The theory of the structure of Perovskite oxide was given by Goldschmidt and in this theory, the formation of Perovskite structure is determined by its tolerance factor (t). That must be satisfied the following equation

$$t = \frac{(rA+ro)}{\sqrt{2}(rB+ro)} \quad \text{.....1}$$

Where, rA, rB and rO are the ionic radii of the A, B (cation), and O (anion).In equation 1 the tolerance factor explains the range of relative size for which Perovskite structure is stable. The geometry of Perovskite oxide depends upon the tolerance factor strongly, the structure of Perovskite will be cubic if the $0.95 \leq t \leq 1.0$. It was observed that compounds having a tolerance factor in the range $0.95 < t \leq 1.0$ will be non-ferroelectric with distorted structure while those with ≥1 are ferroelectric and hexagonal. (Yadava et al. 2017) The value of tolerance factor if < 0.75 the compound does not crystallite in the Perovskite structure. The complex perovskite having the general formula $AA'_3B_4O_{12}$ where A and A'exist at the corner of the cubic lattice, B occupied at body-centered of the cubic lattice, and oxygen is occupied at the face-centered of the cubic lattice. The most widely known perovskite is $CaCu_3Ti_4O_{12}$ complex perovskite oxide which shows a very interesting dielectric constant that was responsible for various applications such as a capacitor, memory devices, microelectronic devices, etc.(Fang et al. 2004),(Huijben et al. 2006),(Huízar-Félix et al. 2012 p. 5) The structure of $CaCu_3Ti_4O_{12}$ is derived from the cubic perovskite (ABO_3) by an octahedral tilt distortion caused by size mismatch and the nature of the A cations. (Demmig-Adams and Adams 2006)The TiO_6 octahedral tilt to produce a structure where three-quarters of the A sites have square–planar coordination and are occupied by Jahn-Teller Cu^{2+} ions. The remaining quarters of the sites are occupied by Ca and have

12 fold coordination. Electroceramic calcium copper titanates ($CaCu_3Ti_4O_{12}$, CCTO), with high dielectric permittivities (ε) of approximately 10^5, respectively, for single crystal and bulk materials, are produced for several well-established and emerging applications such as a resonator, capacitor, and sensor. (Fang and Liu 2005 p. 12),(Ferrarelli et al. 2006 p. 12) These applications take advantage of the unique properties achieved through the structure and properties of CCTO. (Zhuk et al. 2018),(Desu and Vijay 1995),(Fang et al. 2004), This review comprehensively focuses on the primary processing routes, effect of impurity, dielectric permittivity, and deposition technique used for the processing of electroceramics along with their chemical composition and micro and nanostructures.(Bielański et al. 1957),(Bochu et al. 1979 p. 12),(Boulahya et al. 2017) Emphasis is given to versatile and basic approaches that allow one to control the microstructural features that ultimately determine the properties of the CCTO ceramic. Despite the intensive research in this area, none of the studies available in the literature provides all the possibly relevant information about CCTO fabrication, structure, the factors influencing its dielectric properties, CCTO immobilization, and sensing applications. (Ahmadipour et al. 2016) ,(AURIVILLIUS 1949 p. 9)

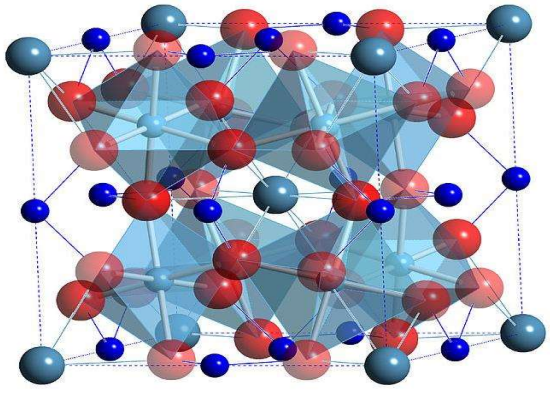

Figure 1.2. Structure of $CaCu_3Ti_4O_{12}$ shown as TiO_6 octahedral, Cu atoms bonded to four oxygen atoms, and large Ca atoms without bonds. (Dsexton1988)

There is a lot of giant dielectrics and ferroelectric material are well know such as $Pb(Mg_{1/3}Nb_{2/3})O3$ (PMN). has a high dielectric constant1000 to20000 but these materials are not eco-friendly. The complex types of perovskite material are recorded with the highly giant dielectric constant of material are $ACu_3Ti_4O_{12}$ which are eco-friendly as well as a giant dielectric constant this leads to important applications. (Badr et al. 2011)$CaTiO_3$ is widely used as a wireless device in electronic ceramic manufacturers and $BaTiO_3$ was a ferroelectric, piezoelectric, and insulating material is broadly used as high dielectric permittivity, low dielectric loss. (Galasso 2013),(Gautam et al. 2016) Whereas, $SrTiO_3$ was received much attention both theoretically and experimentally concerning its defect chemistry and radiation resistance. Nowadays, the structural properties of perovskite including order-disorder effects and the formation of defects and impurities that can tailor the electronic and Physico-chemical properties. (Lettieri et al. 2000 p. 3),(Ferrarelli et al. 2006),(Li et al. 2010) The property of these perovskite oxides may be modified to a novel system with a unique characteristic. (Homes et al. 2001) Over the last decade, extensive experimental and theoretical work on perovskite-based materials has demonstrated a strong interrelationship between distortions of the crystal structure and many processes and phenomena such as photoluminescence, ferroelectric, piezoelectric, and pyroelectric properties. Barium titanate is a well-known ferroelectric and multilayered dielectric material. The discovery of barium titanate was discovered by the Second World War (1941-1944) in U.S.A, Russia, and Japan firstly.$BaTiO_3$ was synthesized by BaO doped TiO_2 for increasing the dielectric constant. The Erie and Resistor company observed that the dielectric constant of $BaTiO_3$ has ten-time greater than TiO_2.$BaTiO_3$ was detailed studies were done by Miyae and Ueda in 1946.(Hamid et al. 2006) It was observed that the curie temperature of $BaTiO_3$ was 120 °C displays tetragonal to cubic phase transition which causes a significant dielectric constant. The

dielectric constant of the polycrystalline ceramic material depends upon the grain size. (Gautam et al. 2017),(Goudochnikov and Bell 2007) The grain size of polycrystalline was observed at 1 μm. This type of increment of dielectric constant was due to the twin's behavior of polycrystals and a decrease in the grain size. (Bueno et al. 2008),(Davies et al. 2008),(Dawber et al. 2005) .

1.1 High dielectric constant ABO_3 Perovskite

(a) Calcium Titanate $CaTiO_3$

It is pointed out that at room temperature the behavior of $CaTiO_3$ is paraelectric. When doped cation the internal boundary layer effect gets increases so the dielectric constant is also increased. The ceramic materials are very sensitive by doping of cation or anion and sintering process. The symmetry of $CaTiO_3$ is strongly dependent upon the temperature and at room temperature, it is orthorhombic but became tetragonal symmetry at 600°C, which converts into cubic symmetry at 1000°C. The conductivities of the oxidizing atmosphere at 130°C displays the p-type semiconductor behavior. (Ali and Yashima 2005)

(b) Barium Titanate (BaTiO3)

It is pointed out that the high dielectric constant of this ceramic is mainly due to its ferroelectric behavior. The radii of Barium and Oxygen almost the same. Titanium ion is occupied at the body-centered of the cubic lattice which is surrounded by six oxygen atoms.TiO_6 octahedra in barium titanate shifted either up or down, this is responsible for ferroelectricity. It is observed that in $BaTiO_3$, Titanium exists in a +4 oxidation state and laying d-orbital of titanium originates electronic polarization and atomic originates around it. It was observed that on cooling there are three phases of transition recorded. These transitions affect the direction of spontaneous polarization from one phase to the other.$BaTiO_3$ shows a hexagonal structure when its temperature increases up to

1450°C.BaTiO3 at below 1450°C exist in a cubic form which is paraelectric.$BaTiO_3$ at room temperature exists tetragonal structure with axial approximately 1.012 strong temperature-dependent dielectric constants at curie temperature. (Smith et al. 2008 p. 3),(A. Molina-García and V. Rees 2016) ,(Bassat et al. 2013 p. 2) .

(c) $SrTiO_3$

It is mainly used as high-temperature superconductor thin film in photocatalyst of the water Oxygen sensor and magneto hydrodynamic operators memory devices optical processes. (Zhuk et al. 2018) It is observed that the oxygen vacancy is responsible for n-Type conductivity. $SrTiO_3$ at room temperature cubical structure with band gap 3.2 eV, and paraelectric. It is observed that when trivalent rare earth metal ion-doped strontium titanate displays high dielectric constant and relaxor behavior. (Banerjee et al. 2006), It is observed that the dielectric properties of $SrTiO_3$ are about 300. Yttrium doping improves it up to 18000. (Sharma et al. 2014),(Allison 2007),(Amow et al. 2006) ,(Camargo et al. 2009),(Carrasco et al. 2006)

1.3 APPLICATIONS OF PEROVSKITE OXIDES:

Since the perovskite structure can accommodate a variety of cations and anions that change its structure and properties, deep interest in this class of materials has emerged. These compounds form a large group of dielectric materials having ferroelectric, antiferroelectric, and paraelectric behavior at room temperature. Members of the perovskite family of type I ($A1+B_5+O_3$) find applications in electro-optic devices due to their large electro-optic coefficients at room temperature. Due to large acoustic coefficients at room temperature, $KNbO_3$ and $KTaO_3$ of the above family are used in acousto-optic devices $LiNbO_3$, $LiTaO_3$, and KTaO3 are used as electro-optic materials, microwave surface acoustic devices, and holography memory devices. Compounds of

family $A_2+B_4+O_3$ exhibit piezoelectric as well as ferroelectric properties at room temperature. They are used as piezoelectric transducers, phonograph picks up, air transducers, instrument transducers, underwater sound and ultrasonic power wave filters, delay line transducers, gas lighter elements, dynamic and blast gauges accelerometers, and high voltage sources. They are also used for sound transmission and reception, ultrasonic cleaning devices, information storage in electronic computers, and dielectric amplifiers. (Chandler et al. 1993) Another important perovskite oxide of this family is $SrTiO_3$ which can be used as grain boundary barrier layer capacitors (GBBLC) and positive temperature coefficient (PTC) thermistors. It also finds application in the photolysis of water, as a gas sensor and magneto hydrodynamic (MHD) applications. Thin films of $BaSnO_3$ deposited on Al_2O_3 substrate are used for 21 sensing CO_2 and nitrogen dioxide gases at constant partial pressure. $SrSnO_3$ is used as a humidity sensing material. $BaSnO_3$ and its solid solutions with titanates have also found applications in the fabrication of ceramic boundary layer capacitors. Barium-based B-site substituted compounds are used as microwave resonators, in cellophane. Pb-based B-site substituted compounds are used as multilayer capacitors for miniaturization and in the electronic industry.

Table.1.1. An example of some perovskite explains property application and its use.

Compounds	**Typical property**	**Application**	**Used**
$BaTiO_3$, $PdTiO_3$	Ferromagnetic property Piezoelectricity and high dielectric constant.	Multilayer ceramic capacitors (MLCCs), PTCR resistors, and embedded capacitance.	Most widely used dielectric ceramic T_C = 125°C

(Ba Sr)TiO_3, (Bi, Na)TiO_3	Non-Linear dielectric properties.	Tunable microwave devices.	Used in the para-electric state.
Pb(Zr, Ti)O_3	Ferromagnetic property Piezoelectricity.	Piezoelectric transducers actuators and ferroelectric memories.	PZT most successful piezoelectric material.
$Bi_4Ti_3O_{12}$	Ferroelectric with high Curie temperature.	High-temperature actuators and Ferroelectric Properties.	Aurivillius compound T_C = 675°C
$(K_{0.5}Na_{0.5})NbO_3$, $Na_{0.5}Bi_{0.5}TiO_3$	Ferromagnetic property Piezoelectricity.	Lead-free piezo-ceramics.	Performances are not yet comparable to PZT but rapid progress.
$SrFeO_3$, $LaCoO_3$	Electrical conductivity.	Alternative dielectric materials and Internal barrier layer capacitors.	Multifunctional material.
$BiFeO_3$, $LaMnO_3$	Magnetic property.	Magnetic field detectors, Memories.	Most investigated multi ferroic compound. T_C = 850°C
$LaCoO_3$, $BaCuO_3$	Catalytic property.	Cathode material in SOFCs and oxygen separation membranes.	Used for Solid Oxide Fuel Cells cathodes.
$LaAlO_3$, $YAlO_3$	Host materials for rare-earth luminescent ions.	Lasers Substrates for epitaxial film deposition.	

Dielectric (or dielectric material) is an electrical insulator that can be polarized by an applied electric field. It is pointed out that a dielectric material is positioned in an electric field then the flowing of electric current does not take place through the material. It is pointed out that when the electricity does not flow through the material

only slightly shift from its average equilibrium positions causing dielectric polarization. By causing this phenomenon in which there is developed dielectric polarization, the positive charge shifted to the direction of the field and negative charges shifted to the opposite direction field. (For example, if the positive charges of dielectric polarization shifted the x-axis then negative charges shifted to the y-axis. This type of situation creates an electric field in the semiconducting material. It is noteworthy that if the molecule bonded with the weakly bonded molecule then the dielectric material not only polarized but also reorient. In this situation, they will be aligned to the symmetry axes to the field. The dielectric material is very used full in microelectronic devices. The dielectric properties of materials study are very important in the dissipation of electric and magnetic energy.(Kato et al. 2004),(Kestigian et al. 1957 p. 2),(Kharton et al. 2001) This study also very important in the explanation of electronics,optics,solid-state physics and cell biophysics .(Khenata et al. 2005),(Kim et al. 2006),(Liu et al. 2019),(Yu et al. 2018),(Kim et al. 2014)

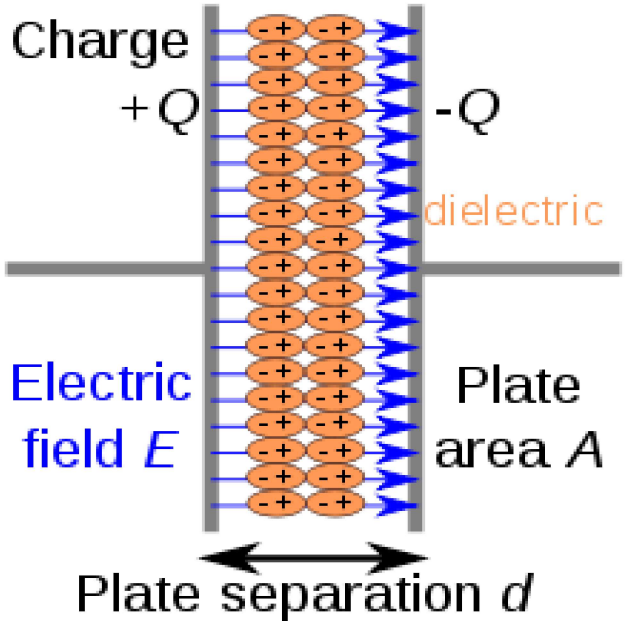

Figure 1.3. Shows the dielectric material which are polarized by electric fields (Arthur R.vonHippel)

1.4. Complex perovskite

The general formula of complex perovskite oxide $(A'A'')(B'B'')O_3$ which is founded a variety of technological applications. The structure and configuration of this type of complex perovskite oxide critical open up a variety of applications by doping homo or heteroatom. (Dubey et al. 2011 p. 12),(Ezhilvalavan and Tseng 2000),(Hao et al. 2009),(Hardy et al. 2004),(Heiland 1954)In this type of perovskite oxide, A exist divalent species but in the case of lanthanide, transition metal ions, trivalent species also exist like Al^{+3}, Ti^{+3}, and Fe^{+3}, La^{+3},Ce^{+3}.On the other hand in complex perovskite at the B site, tetravalent species exist like Ti^{+4}, Mn^{+4},Fe^{+4}, Nb^{+4},W^{+4}.In this complex perovskite oxide, the size of A is greater than that of B usually. It is also attracting the result of dielectric and magnetic properties. The complex perovskite explains the latitude of both ions by which a great deal over the control properties.(Kuo et al. 2001),(Lee et al. 2000),(Lettieri et al. 2000 p. 3) There is some additional perovskite oxide also known which has general formula A_3BX and BAX_3 known to homologous series to as $A_{n+1}B_nO_{3n+1}$,$A_nB_nO_{3n+1}$,(Dion et al. 1981) ,(Holtzworth-Munroe and Jacobson 1985) ,$Bi_2A_{n-1}B_nO_{3n+3}$ (Aurivillius series) [B. Aurivillius(1949), B. Aurivillius(1950), B. Aurivillius(1951)].It is also recorded that the structure of some anion deficient perovskite $A_nB_nO_{3n-2}$ and which is related to ABO_3 perovskite. It is also explained by Ruddlesden-Popper and Dion-Jacobson in a variety of applications of perovskite oxide such as in superconductors, multiferroic magneto resistant materials, ionic conductors, ferroelectrics, the amount of defect, and their mutual interaction. There are some examples of complex perovskite such as. $CaCu_3Ti_4O_{12}$ (CCTO), $CaCu_2Mn_1Ti_4O_{12}$ (CCMTO), $CaCu_{2.9}Mn_{0.1}T_{3.9}Mn_{0.1}O_{12}$ (CCMTMO), $CaCu_3Ti_{3.9}Mn_{0.1}O_{12}$ (CCTMO) .

1.5. Ceramic Materials

These materials are classified into two categories name inorganic and non – metallic materials. These materials are very important, used every day in our life. The properties of these materials are found a different type such as opaque weak, strong, and transparent, insulator, conductor and semiconductor, friable and tough, polycrystalline, single crystal, and composites, high melting, and low melting, etc.(Jang et al. 2002)It is well known that the preparation of ceramic materials was to be found with different methods such as hydrothermal method,sol-gel method, solid-state route, and semi-wet route.(Jacobson et al. 2002) The properties of ceramic are that these show excellent insulating properties. These materials have the capability that they do not allow to path electric current even a very strong field. These materials are also used in semiconductors. There are some ceramic materials are discovered that do not conduct electricity but apply internal charge polarisation and used in-store an electrical charge in capacitors (Richerson and Lee 1992)Examples of electro-ceramics like Zinc oxide for varistors, lead zirconium titanate (PZT) for piezo-electrics, barium titanate for capacitors and lead lanthanum zirconium titanate (PLZT), tin oxide as gas sensors, used for electro-optic devices. (Kuczenski and Segal 1989),(Cabuk et al. 2007),(Cain and Stewart 2014)

Table.1.2. There are physical properties and applications of some ceramic materials.

Material	**Properties**	**Application**
$BaTiO_3$	high breakdown voltage Change of resistance with temperature, high permittivity	Capacitors Thermistors

PLZT	Change of birefringence with field	Electro-optics
PZT	Change of polarization with temperature	Pyroelectrics
$LiNbO_3$	High piezoelectric coefficients	Piezoelectric, Transducers
ZrO_2	Ionic conductivity	Gas sensors
Ferrites	Permeability, coercive field	Magnets
Al_2O_3, AIN, BeO_3	High thermal Conductivity, Low permittivity	Packaging, Substrates

1.5. Composite Material

The definition of composite materials, these are the mixture of two or more materials ((fillers, binder, and reinforcement) of different compositions. In other words, composite materials are called composition of materials or shortened to composites. The physical and chemical properties of composite materials are always different. It pointed out that when composite include strong ply carrying material is known as reinforcement and weaker materials are called matrix. Composite materials are very important in industrial applications for their outstanding resistance to chemicals and most forms of corrosion. It is pointed out that the composite materials are very useful in a variety of applications due to they have unique properties i.e; low mass, low weight, technological possibilities, and matchless manufacturing (Satyanarayana et al. 1990),(Pathania et al. 2009) It is well known that the dielectric constant and tangent loss depend upon temperature and frequency. The composite materials are very useful in electrical applications such as chemical properties, terminals, circuit boards, connectors, switches, etc. Composite materials have excellent mechanical, electrical. Composite materials are also used in part of the aerospace and automobile industries.

1.6. Capacitors

It is the component that has the capability of stored energy in the form of an electric charge generates a potential in the form of across its plates for example a small rechargeable battery. The properties of capacitors are they quickly release energy. The capacitor mainly consists of two or more parallel conducting plates, plates do not touch each other. The conducting plates are electrically far by air or good insulating materials mica, ceramic, plastic waxed paper, ceramic and liquid gel. The material separates into two conducting plates called dielectric. It is pointed out that the potential between two conductors, a static electric field develops across the dielectric is mainly due to an alignment of charges in the dielectric. It is pointed out that in the two conducting plates two opposite charges separated name positive charges and negative charges. The energy of the capacitor is store in the form electrostatic field. Figure 1.2 shows the mechanism of working of the capacitor in the circuit, including the alignment of charges in the dielectric materials.

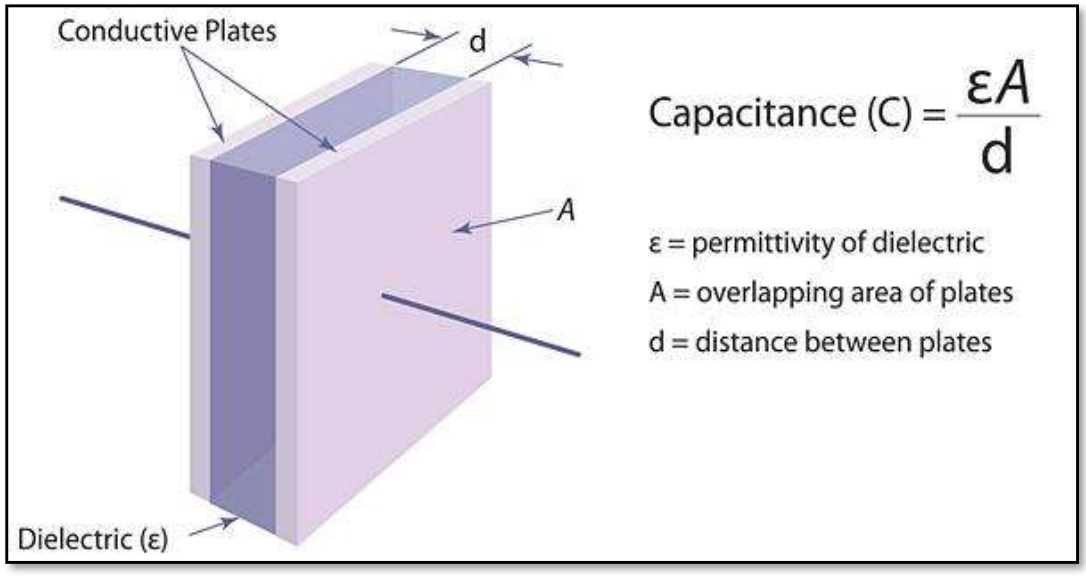

Figure 1.4. displays parallel plate capacitors in the circuit, including the alignment of charges in the dielectric material (Mark Howard (2015).

Equation 1.1 depicts the capacitance of the parallel plate capacitor

$$C = \varepsilon_0 A/d \qquad (1.1)$$

In the above equation, ε_0 (8.854×10^{-12}F/m) is the permittivity of free space. It is pointed out that the dielectric constant of capacitance is higher than it favored for the practical design of embedded capacitors for miniaturization.

1.7. Dielectric Materials

The ceramic material which is a good electric insulator known as the dielectric material. Dielectric and electrical properties of also explained by composites materials. When the electric field is applied to the ceramic materials the current does not pass and a slight dipole has been developed. It is pointed out that positive and negative charges separated which is shown in figure 1.5

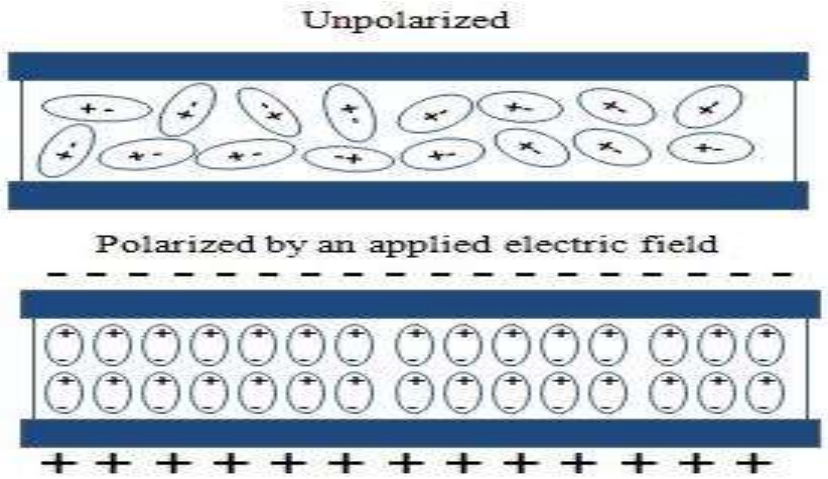

Figure 1.5. Depict the polarized and nonpolarized plates of an applied electric field (Saint Jude (2012)).

Figure 1.5 clearly shows a dipole moment has been developed when the electric field is applied. The dipole moment found per unit volume is called polarization. The dipole moment is directly proportional to the electric field (E). The dielectric

polarization is directly proportional to the applied field. (Boukenter et al. 1988) display in the given below equation

$$P = n\chi eE \qquad (1.2)$$

In the above equation χ_e the dielectric susceptibility and n is a dielectric constant which explains the ability to form dipoles. (Rossouw et al. 2007)It is well known that the dielectric susceptibility is equal to (ε_{r-1}), ε_r is the relative permittivity, the dielectric polarization will be.

$$P = \varepsilon_o E\,(\varepsilon_{r-1}) \qquad (1.3)$$

The field that a molecule in their ward of a dielectric recognized between the plates of a charged condenser virtually experiences is known to be larger than the applied field. This is related to the polarization which exhibits on the surfaces of the dielectric. The actual field of a molecule is called the local field (E_{loc}). The dipole moment for a molecule by the local field is given by (Garmong and Shepard 1971)

$$P_{mol} = \alpha' E_{loc} \qquad (1.4)$$

where $P_{mol}$is a moment and$\alpha'$is called molecular polarizability. For dielectrics containing N molecules per unit volume, the total dipole moment or polarization is:

$$P = N\,\alpha' E_{loc} \qquad (1.5)$$

Substituting Equation (1.4) in Equation (1.5) gives

$$\chi_e=(\varepsilon_{r-1}) = P/\,\varepsilon_o E_{loc}= N\,\alpha' E_{loc}/\,\varepsilon_o E \qquad (1.6)$$

It is pointed out that when the dielectric material is present it reduces the effectiveness and various polarizations such as orientation (dipolar) polarization, Electronic polarization, atomic or ionic polarization, space charge polarization. The total polarization P of the dielectric material, and is given as:

$$P = P_{electronic} + P_{ionic} + P_{molecular} + P_{interfacial}$$

1.8. Electronic Polarization

This type of polarization is found the all-dielectric materials. When an individual atom feels on it surrounding electrical fields the nucleus, there will be a slight dipole moment developed. In this situation nucleus very slightly shifted to the positive electrode and very slightly shifted to the negative electrode then the atom accrued a dipole moment (P)

$$P = \alpha' E$$

The electric field which was to be applied to the atom if it removes then quickly dipole moment disappear.In electronic polarization displacement of charge very less. The electronic polarization is very less as compared to other mechanisms.

1.9. Orientation Polarization

The types of polarization occur when a system is composed of heteronuclear molecules. This type of polarization occurs permanently in the system. Examples of these types H_2S, HBr, CH_3CH_2Br, HI).For the H_2S molecule in this system both hydrogen are covalently bonded but sulphure is more electronegative than both hydrogens so the partial positive charge creates in hydrogen and sulphure feels partial negative charge so here the net charge is not equal to zero. The system has a permanent dipole moment when the electric field applies than then the positive charge shifted to the negative electrode and negative charges shifted to positive electrodes. It is not valid for all the systems that are composed of heteronuclear molecules example CO_2 is a non-polar molecule .H_2S polar molecule because it bent shape structure and it dipole moment not is equal to zero. It is noteworthy that orientation polarization is dominant over electronic polarization. In the orientation polarization, larger displacement creates

on the system. In the solid system, they are tightly bounded but orientation polarization occurs. Orientation types of polarization are very important in liquids and gases. In this type of polarization when thermal heating takes place which more effective on vibration as the temperature decreases give rise to dielectric constant. The dielectric constant is also dependent on temperature.

1.10.Space Charge Polarization

These types of polarization are very random. This type of polarization is caused by cosmic radiation, thermal deterioration process.

1.11. Atomic or Ionic Polarization

This type of polarization occurs when atom (ion) displacement takes place within a crystal structure. In the crystal system when an electric field is applied, stretch the bond between ions or this will change the moment of the molecule. It is pointed out that the atomic polarization effect depends upon crystal structure. The presence of solid solution and other coefficients

Table 1.3. Shows polarization mechanism of dielectric materials

Polarization Mechanism					
Type of polarization	**No E field** (E=0)	**Local Field E** (E≠0)	**Case where it is Observed**	**Frequency range where it is predominant**	**Strength of Polarization**
Electronic Polarization	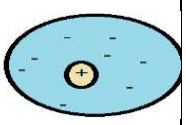	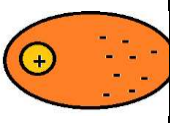	Neutral atoms	~ 10^{15} Hz	This types of polarization Very weak

Atomic or Ionic polarization	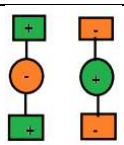	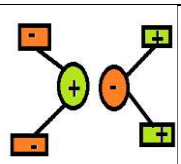	Ionic species	10^{12} to 10^{13}Hz	Very Strong
Molecular or Orientation or Dipolar Polarization		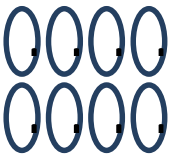	Molecules with permanent dipole moment	10^{11} to 10^{12} Hz	Very Weak
Interfacial Polarization	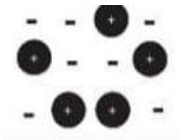		Heterogeneous Systems	10^{-3} to 10^{3} Hz	Very very strong

1.12. Dielectric Constant

The term dielectric constant is also known as **relative permittivity** or **specific inductive capacity.** The dielectric materials are those materials that are electrical insulators but when the field applies to the system can be polarized. In the dielectric constant, an insulating material is put between two flat plats. the properties of the flat are one plate became a positive charge bear and the other plate becomes a negative charge. When an electric field is applied then they can be polarized between two conducting plates The relative permittivity is denoted by the Greek letter kappa, κ, which is simply expressed as $\kappa = C/C_0$. (Richerson and Lee 1992) .Dielectric constant or

relative permittivity is a number unit less dimension. The material which has low dielectric constant is very important used in the electrical insulator. Materials with a high dielectric constant are applicable in the capacitor and other microelectronic devices. Materials with a high dielectric constant are favored in the design of embedded capacitors to achieve high energy density in a given space and further miniaturization. In another field relative permittivity (k) can be represented as

$$k = \varepsilon' - j\varepsilon'' = \varepsilon_0\varepsilon_r - j\varepsilon''$$

In the above equation, ε' denoted to the real dielectric constant, and ε'' expressed to the imaginary dielectric constant. The real dielectric constant (ε') is directly associated with the material. The real dielectric constant is mainly directly associated with frequency, temperature, voltage, and time. The polarization of all has a characteristic mechanism. The dielectric constant of materials depends upon frequency, temperature, voltage, and time. (Bai et al. 2000) ,(Balamurugaraj et al. 2013),(Cohen et al. 2003 p. 12),(Koops 1951),(Kretly et al. 2003),(Kumar and Rao 2012)

1.13. Dielectric Loss or tangent loss

Dielectric loss is a material property of the dielectric and is a measure of energy loss of the dielectric during ac operation. (da Conceição et al. 2011)The tangent loss is a result of distortion, interfacial dipolar, and conduction losses. Dielectric loss is also known as tangent loss (tanδ) and it is defined as

$$tan\delta = \varepsilon''\varepsilon' + \sigma 2\pi f\varepsilon$$

Where $\varepsilon'$is the real part of dielectric permittivity, $\varepsilon''$is the imaginary part of dielectric permittivity and σ denotes to the electrical conductivity of the material and f is denotes to the frequency. . Energy loss (W) which is defined as the energy dissipated in a dielectric material is proportional to the loss tangent and is expressed as

$$W \approx \pi\varepsilon' E2f tan\delta$$

Where E denotes the electric field strength, expressed as the frequency. From the above equation, it is clear that for the capacitor application low tangent loss of materials is preferred to minimize the energy dissipation factor. (Mannath et al. 2004),(Joanni et al. 2008),(Jonker 1954)

1.14. Impedance

This method is excellent for determining the electrical properties of the materials and their interfaces with electronically conducting electrodes. This method may examine the dynamics of bound or mobile charge in the bulk region of any kind of liquid materials or solid. This method is always used to investigate the semiconducting, ionic, dielectric and mixed electronic–ionic. It is also useful for determining the migration of charges carrier across the grain and grain boundaries. This method applied a single–frequency current to the interface and determining the amplitude and phase shift or real and imaginary parts of the resulting current at that frequency using analog in the circuit. This is the most important technique in which the basic concept is based on analyzing the ac response of a system to a sinusoidal perturbation.

The powerful impedance spectroscopy is mainly categorized in two types (i) Materials used in it self such as dielectric constant, conductivity, equilibrium concentrations of the charged species, mobilities of charges, and bulk generation–recombination rates (ii) materials used in the electrode-material interface, such as capacitance, etc.

Impedance spectroscopy has very important in modern advances in electronic automation. It is very important to note that a large number of critical equipment has been developed to measure and analyze the frequency response to small–amplitude ac signals in the range between 10^{-6} -10^{-4} Hz . By this spectra, a large number of microelectronic devices have been developed such as industrial quality control of paints,

computers chips, electroplating, emulsions thin-film technology, the mechanical performance of engines, materials fabrication, corrosion, and so on. The impedance spectra have two components real (Z') and imaginary (Z″). By this spectral response, many types of material can be synthesized such as inductors, capacitors, resistors, and other elements. Transforms is also an example due to the response of impedance spectra.

Table1.4. The high dielectric constant of few oxide compounds

S. No.	Compound	Dielectric constant	Reference
1.	$CaCu_2Mn_1Ti_4O_{12}$	5×10^3	(Kumar et al. 2020b)
2.	$Bi_{2/3}Cu_3Ti_4O_{12}$	2.9×10^4	(Gautam et al. 2016)
3.	$Y_{2/3}Cu_3Ti_4O_{12}$	8434	(Sharma et al. 2014)
4.	$Y_{2/3}Cu_{2.90}Zn_{0.1}Ti_4O_{12}$	1.85×10^4	(Sharma et al. 2018 p. 2)
5.	$CaCu_3Ti_4O_{12}$	10^4	(Kumar et al. 2020b)
6.	$BaFe_{11.95}Co_{0.05}O_{19}$	2.3×10^3	(Kumar et al. 2020a)
7.	$CaCu_3Ti_{4-x}Sn_xO_{12}$	6.51×10^4	(Boonlakhorn and Thongbai 2020)
8.	$0.5Bi_{2/3}Cu_3Ti_4O_{12}$ - $0.5Bi_3LaTi_3O_{12}$	13.94×10^3	(Gautam et al. 2017)
9.	$Ba_6Y_2Ti_4O_{17}$	1.5×10^3	(Yadava et al. 2016)
1	Eu_2CuO_4	5×10^3	(Salame et al. 2014)

0.			
11.	$Bi_4Ti_3O_{12}$-$BaTiO_3$	4.75×10^3	(Singh *et al.*(2020)
12.	$CaCu_{2.9}Zn_{0.1}Ti_4O_{12}$	5971	(Singh et al. 2013)
13.	$Y_{2/3}Cu_3Ti_{3.95}In_{0.05}O_{12}$	5068	(Singh *et al.*2016)
14	$Bi_{0.5}Na_{0.5}TiO_3$	5000	(Lin *et al.*(2004)
15.	$(Ba_{0.95}Ca_{0.05})$ $(Ti_{0.96}Zr_{0.04})O_3$	3910	(Yang et al. 2011)
16.	$SrTiO_3$	2150	(Penn et al. 1997)
17.	$Bi_4Ti_3O_{12}$	1400	(Xiang et al. 2006)

The real parts of the complex dielectric constant shown below

$$\varepsilon' = -Z''/\omega C(Z'^2 + Z''^2)$$

The imaginary part of the complex dielectric constant shown below

$$\varepsilon'' = -Z'/\omega C(Z'^2 + Z''^2)$$

The real parts of complex electric modulus are shown below

$$M' = \omega CZ'' \quad (1.15)$$

Imaginary parts of complex electric modulus shown below

$$M'' = \omega CZ'$$

The loss tangent is given as

$$\tan\delta = \varepsilon'/\varepsilon'' = M''/M$$

the radial frequency ω is shown below

$\omega = 2 \pi f$

with f being the frequency and the vacuum capacitance C is given in above

$C = \varepsilon A/d$

with A is the area of the electrode and d is the thickness of the dielectric layer.

1.15 Magnetic Properties

Magnetism is a material attribute that results from the alignment of magnetic moments. A magnetic field is created by the net flow of electric charge and magnetic moments of elementary particles, which operate on other magnetic moments and currents. When a magnetic field is applied, the spin of electrons in the materials tends to align, increasing the magnetic field strength. (Andres et al. 2012),(Koehler and Wollan 1957 p. 3),(Roy et al. 2005),(He et al. 2010),(Markovich et al. 2014),(Rajeswari et al. 1998) This increase is given by the parameter called magnetization (M). The magnetic flux density of the materials is given by the equation

$$B=\mu_0 H+\mu_0 M \qquad (1.15)$$

From the above equation, μ_0 is called the universal constant as the permeability of free space($4\pi \times 10^{-7}$ H/m). In the above equation, H is known as magnetic field strength, M is called Magnetization. The magnetization i.e. net magnetic moment per unit volume of a substance is defined as $M= \chi_m H$ and $\chi_m= \mu_r-1$ .The mathematical symbol χ_m denotes magnetic susceptibility and μ_r represents to relative permeability. Relative permeability μ_r is the ratio of permeability, the measure of the degree to which a material can be magnetized and permeability of the vacuum ie $\mu_r = \mu/\mu_0$. A large number of applications of magnetic materials such as microwave devices, tunnel junction, and magnetic recording media as well as in the video recorder, data storage.

(Hamid et al. 2006), Magnetic materials have a very special types of properties such as high electrical resistivity, low loss, and magnetic coupling. These properties which are shown by materials, properties can be changed by composition and structure. The properties of ceramic material depend upon chemical compositions, particle size, synthesis process, and morphological behavior. It is pointed out that if particle size less than 100 nm then altered in nanoscale in comparison to the bulk material.

1.15.1Origin of magnetism

The materials magnetism is caused by spin and orbital motion around the nucleus of an electron, and they can be magnetic or non-magnetic. Due to the existence of unpaired electrons in the d orbitals, materials such as transition metals tend to create magnets. The quantum number Ms +1/2 or -1/2 represents the spin of a single electron. When an electron's spinning is paired with another in the orbital, their magnetic moments cancel out each other, resulting in a weak magnetic field when the electrons are unpaired as a result; the materials have some magnetic moment.

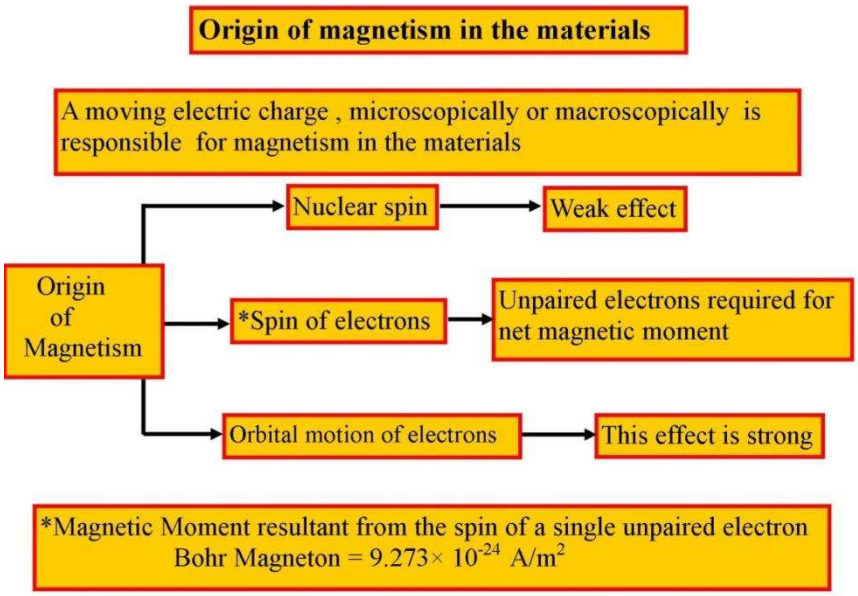

Figure 1.6. Flow chart for the origin of magnetism in the materials.

Magnetic Domain

Magnetic domains are defined as areas within materials where magnetization occurs in a uniform direction. It is pointed out that in material, magnetic movement (or spin of the electron) are randomly oriented at a certain region. In the magnetic domains at a certain area approximately billions of atoms are found in a millimetre size. In the absence of a magnetic field, the spinning of electrons in ferromagnetic materials is random, resulting in a soft substance. In the case of ferromagnetic material magnetized easily but not time of period retain. (Chaudhuri and Mandal 2012),(Chu et al. 2014)In the presence of a magnetic field, the magnetic domains are aligned parallel in the same direction. As a result, the material's net magnetic moment is non-zero and exhibits high magnetization. These materials are hard and have a permanent magnetic moment, which means that their magnetization continues even when the magnetic field is removed. (Andres et al. 2012) ,(Zhao et al. 2004)

Michael Faraday was the first to classify chemicals based magnetic properties in the eighteenth century. Faraday distinguished them as diamagnetic or paramagnetic, and he did so based on the force exerted on the materials when they were placed in an inhomogeneous magnetic field. Table.1.8.

Table 1.8 A summary of the different types of magnetic behavior.

Types of magnetism	Susceptibility	Atomic/Magnetic behaviors		Example
Paramagnetism	Small & positive, $+10^{-5}$ to $+10^{-3}0^{-5}$	Atoms have randomly oriented		O_2, NO B_2,etc.

		magnetic moments	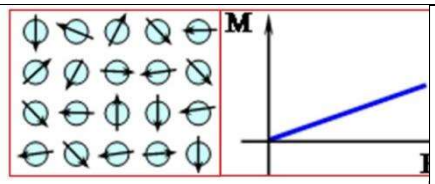	
Diamagnetism	Small & negative, -10^{-6} to 1	Atoms have no magnetic moments	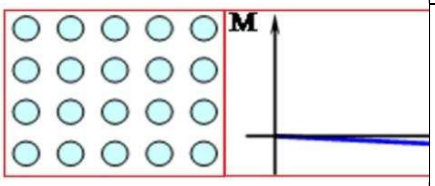	Au, Cu, Hg etc.
Anti-ferromagnetism	Small & Positive $+10^{-5}$ to $+10^{-3}$	Atoms have mixed parallel and anti parallel aligned magnetic moments	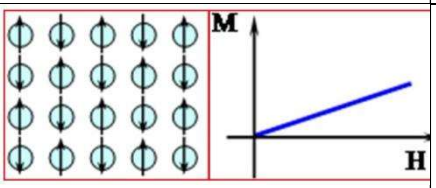	Mn, Cr, MnO, NiO etc.
Ferromagnetism	Large & positive (below Tc), Function of applied field, Microstructure dependent	Atoms have parallel aligned magnetic moments	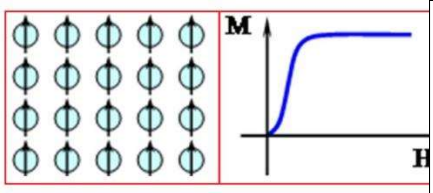	Fe, H, Co, Ni etc.
Ferrimagnetism	Large & positive (~3) Function of applied field, Microstructure dependent	Atoms have anti parallel aligned magnetic moments	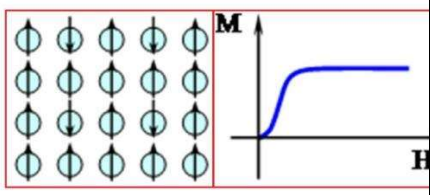	Ba ferrite

1.15.2. Types of magnetic materials

The magnetic materials are classified on the basis of alignment of magnetic moment with or without external magnetic field.

(a) **Paramagnetic**

The materials which have unpaired of an electron called paramagnetic**.** These materials have incomplete cancelation of magnetic dipoles. In paramagnetic materials when in the absence of magnetic field random alignment of magnetic movement. When external fields are applied orientation of magnetic moment towered the field direction large magnetic moment occurred. (Bibes and Barthelemy 2007)It is pointed out that if the temperature of material increases then the randomness of magnetic moment moments also decreases, magnetic susceptibility also decreases. (Awana et al. 2003),(Bowers and Owen 1955).

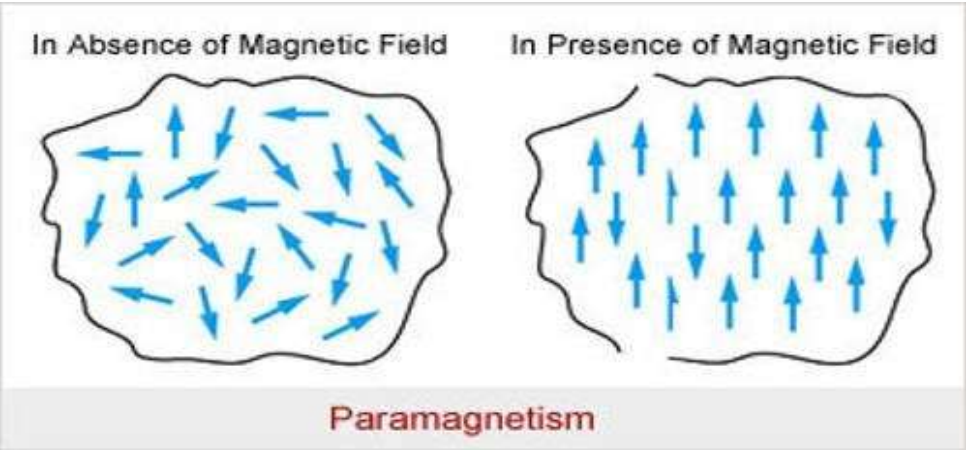

Figure 1.7.shows the Paramagnetic nature of the material in the absence of applied magnetic field and in the presence of the magnetic field.

Curie's law explains the temperature dependant magnetic susceptibility.

$$\chi = {}^{C}/_{T}$$

In the above equation χ denotes to susceptibility, C is denoted to the Curie constant and T is a temperature. It is pointed out that when temperature increases the paramagnetic susceptibility decrease. When the temperature decreases the material became more magnetic Curie's law is only suitable to the system that contains non-interacting magnetic moments and assumed that individual magnetic moment does not interact with each other. Weiss modified Curie's law using the idea of a molecular field.

$$\chi = C/T - \theta \qquad (1.17)$$

The above equation is called known as the Curie-Weiss law, where θ is a measure of the strength of the magnetic interaction. At normal temperatures and in a moderate magnetic field, the paramagnetic substances have less magnetic susceptibility than diamagnetic materials. Magnetic susceptibility will be independent of the applied magnetic field if the temperature is low or the magnetic field is strong. (Kumar et al. 2020c),(Maaz et al. 2010)

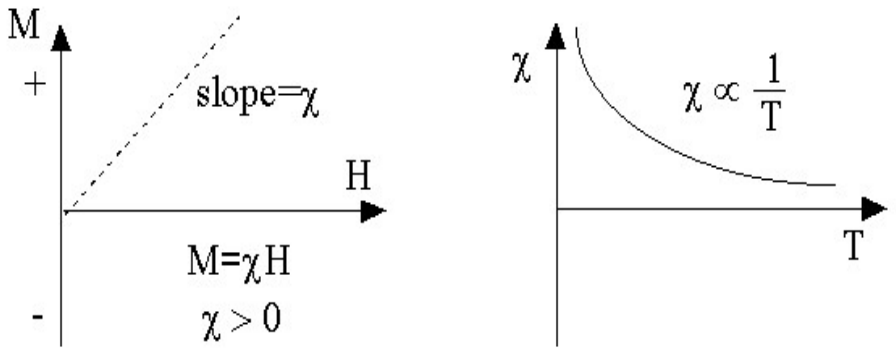

Figure 1.8 Paramagnetic structure

(a) Diamagnetic

Diamagnetic materials are that material which are weakly repelled by an external magnetic field. A magnetic field given to them induces an induced magnetic field in the opposite direction, resulting in a repulsive force. Because all of the spins cancel each other out, there is no magnetic moment in these materials. Diamagnetic materials have negative magnetic susceptibility or less than one. These materials do no depend upon the temperature. Only a purely diamagnetic substance exhibits diamagnetic behavior, which is a universal occurrence. The orbital motions of the electrons cause magnetization in this situation. (Ebner and Stroud 1985),(Shamonina and Solymar 2004) .

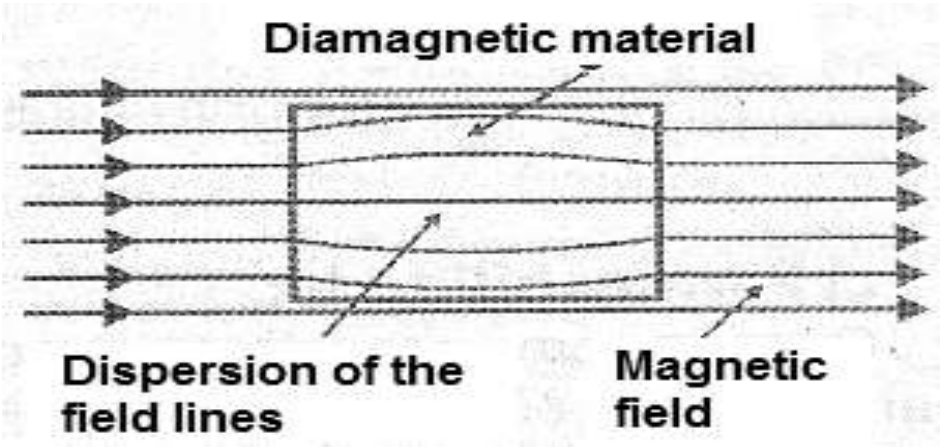

Figure 1.9. Displays the diamagnetic materials disperse the line of force a magnetic field.

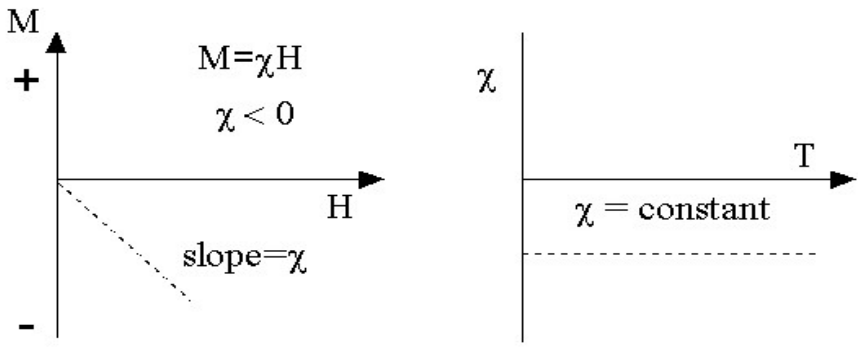

Figure 1.10. Diamagnetic structure

(C)Ferromagnetism

Ferromagnetic substances are those that are strongly attracted by an external magnetic field and can keep their magnetic properties when the external magnetic field is removed. This type of material have unpaired of electron so the magnetic moment of these materials is non-zero. Due to the presence of magnetic domains, they have positive magnetic susceptibility in the direction of the magnetic field and retain a strong magnetic character. (Fava et al. 1997),(Kawasaki et al. 1996), A large number of atoms are aligned parallel in the magnetic field direction in magnetic domains. When these materials are unmagnetized , their domains are randomly orientated and their net magnetic moments are zero. However, in the presence of an external magnetic field, these domains align parallel to each other in the magnetic field's direction. Examples of some ferromagnetic materials Iron, Cobalt, Nickel, etc . (Reed et al. 2001),(Chaudhuri and Mandal 2012) The properties of these materials vary at the Curie temperature (Tc),

with ferromagnetic behavior below Tc and paramagnetic behavior beyond it. (Devan et al. 2007) .

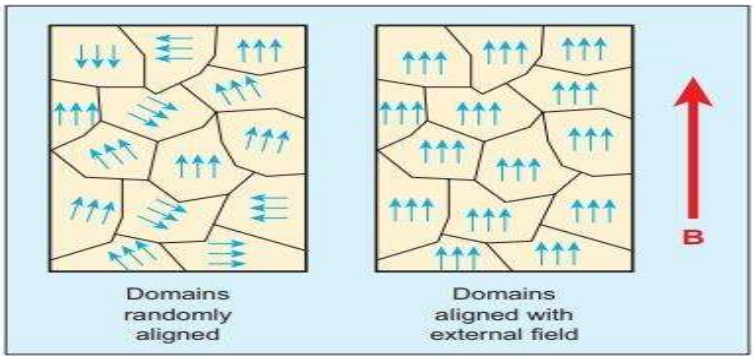

Figure 1.11. Ferromagnetism non-magnetized material and Magnetized material with the corresponding magnetic field .

(iv) Anti-ferromagnetic

Antiferromagnetic materials are similar to ferromagnetic materials, but when a magnetic field is applied and temperatures are below the critical temperature, the alignment of their spins is anti-parallel to one other. Magnetic ordering exists below that temperature which is known as the Neel temperature and vanishes above this temperature, becoming paramagnetic.(Baltz et al. 2018),(Chen et al. 2020),(Sapozhnik et al. 2017) An antiferromagnet's magnetization remains constant below Neel temperature, and the antiparallel spin's alignment is preserved when the external field is eliminated.

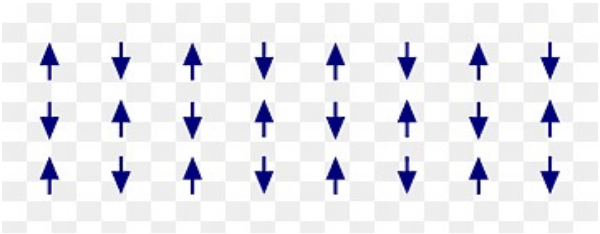

Figure 1.12 Anti-ferromagnetic structure

(V) Ferrimagnetism

This word was given by Nell in 1948. In this type of material, the alignment of magnetic moment in such a way that the moments do not completely cancel out resulting in net magnetization remains at even no external field is applied. For example; Cubic ferrites (iron oxides with the other elements such as nickel, zinc, cobalt and aluminum), Yttrium iron garnet, and hexagonal ferrites such as $Fe_{1-x}S$, pyrrhotite, $PbFe_{12}O_{19}$ and $BaFe_{12}O_{19}$, etc., (Hu et al. 2007),(Shimakawa 2015)

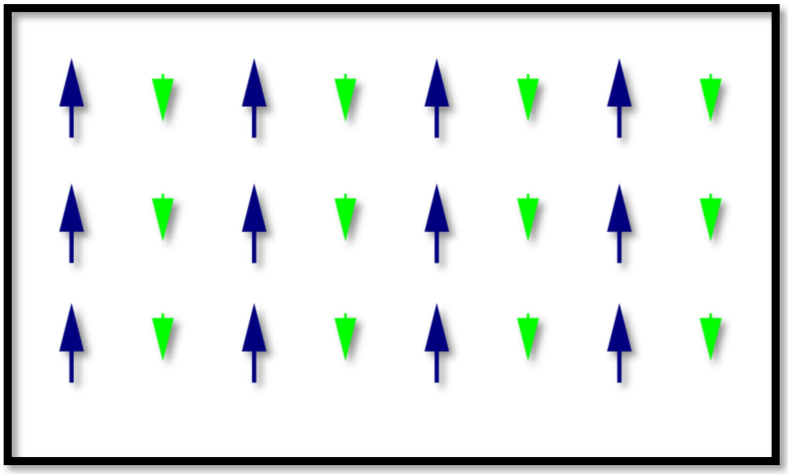

Figure 1.13 Ferrimagnetism structure

(Vi) Griffith's Phase (T_G)

This is the temperature where magnetic properties of the materials show ferromagnetic in paramagnetic regions. This is a susceptibility disorder magnetic disorder. The onset of a Griffiths-like phase has been observed in $CaCu_3Mn_4O_{12}$ means of magnetic susceptibility. We show the growth of a ferromagnetic cluster system characterized by an inverse susceptibility exponent lower than unity at $T_C<T<T_G$ approximately 222 K to 272 K.(Kumar et al. 2020c)It is pointed out that Griffiths-like state is originated by local disorder within the crystallographic structure, stabilized and enhanced by competing intralayer and interlayer magnetic interactions. Both factors

thus promote the segregation of nanometric regions with ferromagnetic interactions. (Nair et al. 2011 p. 6),(Ghorai et al. 2021)

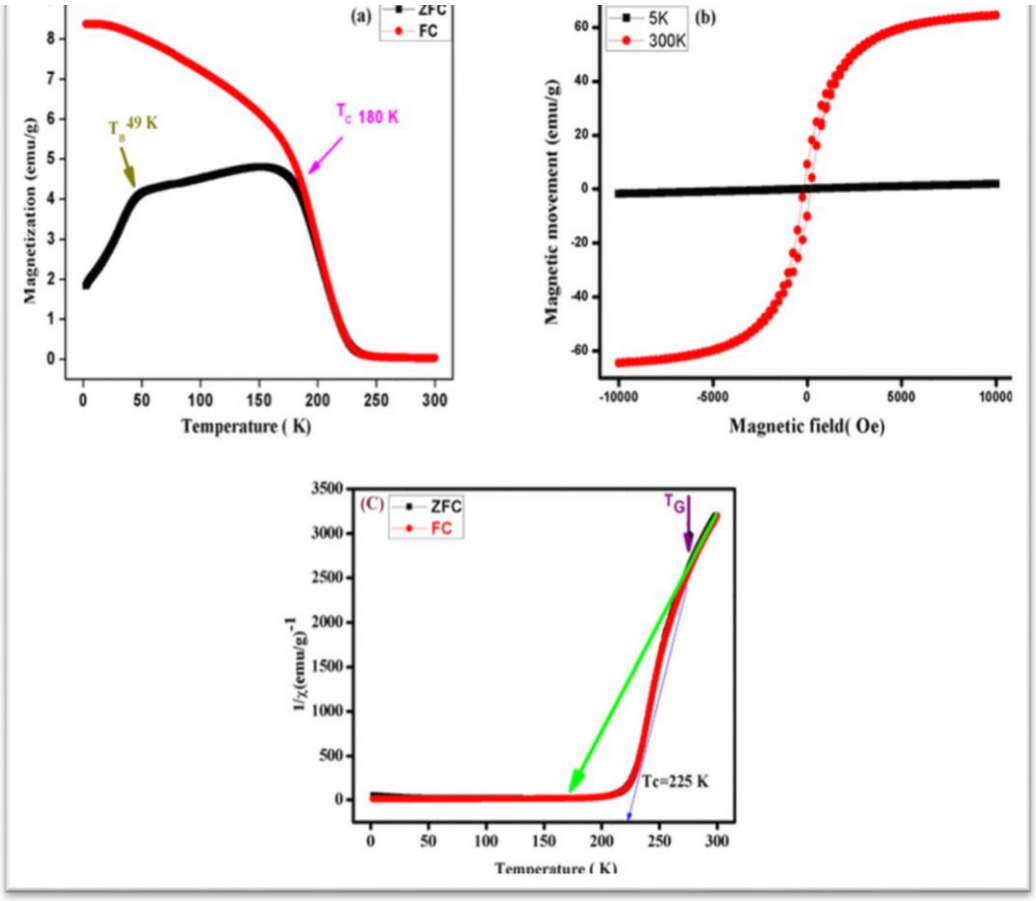

Figure 1.14. (a) Temperature dependence of ZFC and FC magnetization plot, top insert indicates dM /dT vs T **(b)** depicts the M-H hysteresis loop recorded at 5 and 300 k.

(C) Shows inverse magnetic susceptibility $1/\chi$ (T) for CCMO measured in the range of 0 to 300 K. The onset temperatures T_G where $1/\chi$ (T) deviates from the linear temperature dependence (solid green line) are indicated by the arrows, showing the signature of Griffith's Phase behavior.

(VII) Superparamagnetism

This type of properties are observed in small ferromagnetic or ferrimagnetic nanoparticles (NPs). If the size of these nanoparticles is small, the alignment of the magnetic moment of electron randomly flip direction under the influence of temperature. (Kumar et al. 2009) It was discovered in those materials that have a smaller size and number of domains, typically between 10 and 150 nanometers in diameter, and behave as a single magnetic domain. For individual particles, the single domain anisotropy energy equation can be expressed as

$E_{anisotropy}(\alpha)=-KV\cos^2\alpha$

In the above equation K is the uniaxial magnetic anisotropy constant, is the volume of the particle, and α is the angle between the directions of magnetization.

At any given time, superparamagnetic materials can be presumed to be strongly magnetized materials. However, the particles of these materials have zero remanent magnetization and zero coercivity when seen over a sufficiently long period, i.e. higher than 10^{-9} seconds. Furthermore, due to thermal fluctuation, spontaneous demagnetization is found in superparamagnetic materials, resulting in a saturated assembly with no hysteresis and zero coercivity. As a result, these materials have found widespread application in drug delivery, magnetic hyperthermia, and magnetic resonance imaging. Hard disc drive technologies, loudspeakers, suspension systems, and numerous medical applications all use this sort of substance, which may also be found in rocks and living organisms. The blocking temperature (TB) at which the maximum magnetic moment is detected, which varies with particle size and decreases as particle size increases, determines whether the material is ferromagnetic or superparamagnetic. (Knobel et al. 2008) ,(Usov et al. 2021)Material behaves as ferromagnetic below TB

and becomes Superparamagnetic above this temperature. Figure 16 shows the M-H hysteresis curve for paramagnetism , superparamagnetism, and ferromagnetism.

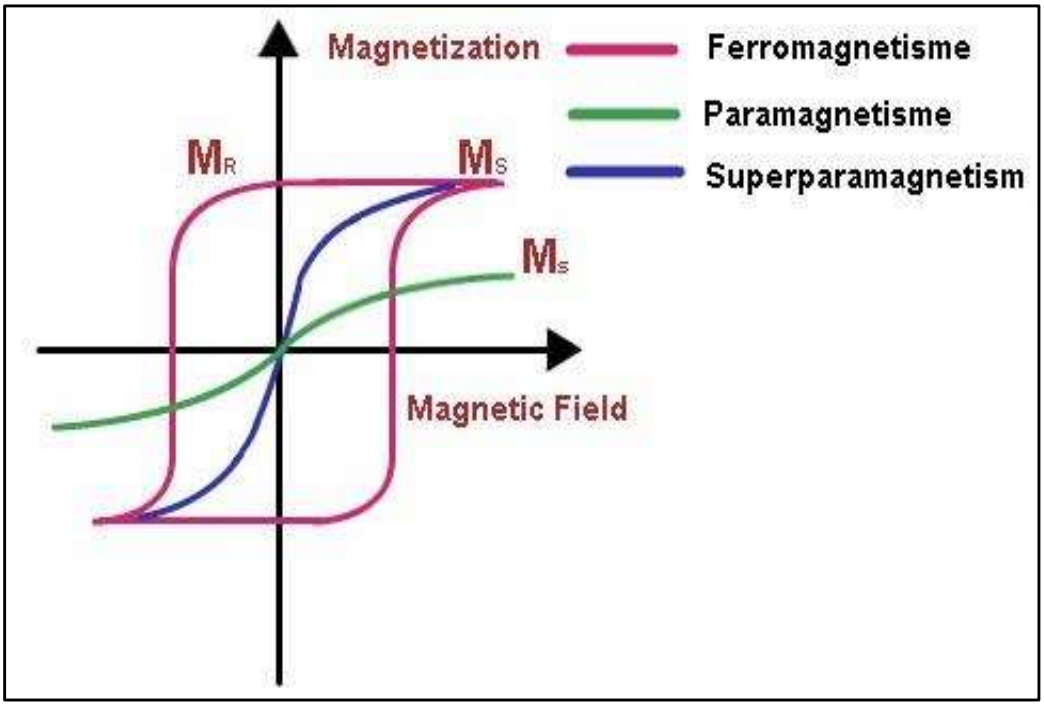

Figure 1.15 M-H hysteresis loop

1.15.3 Hysteresis loop

The hysteresis loop, which shows the relationship between the magnetizing force (H) and the induced magnetic flux density (B), can be used to learn about the magnetic characteristics of materials. It's referred to as the B-H curve, and it's depicted in Figure 1.17. When an external magnetic field is applied to ferromagnetic materials, such as iron, the atomic domains align, and their magnetic characteristics are conserved in the materials when the magnetic field is removed because some of the alignment is kept. The magnet will remain magnetised eternally once it has been magnetized.

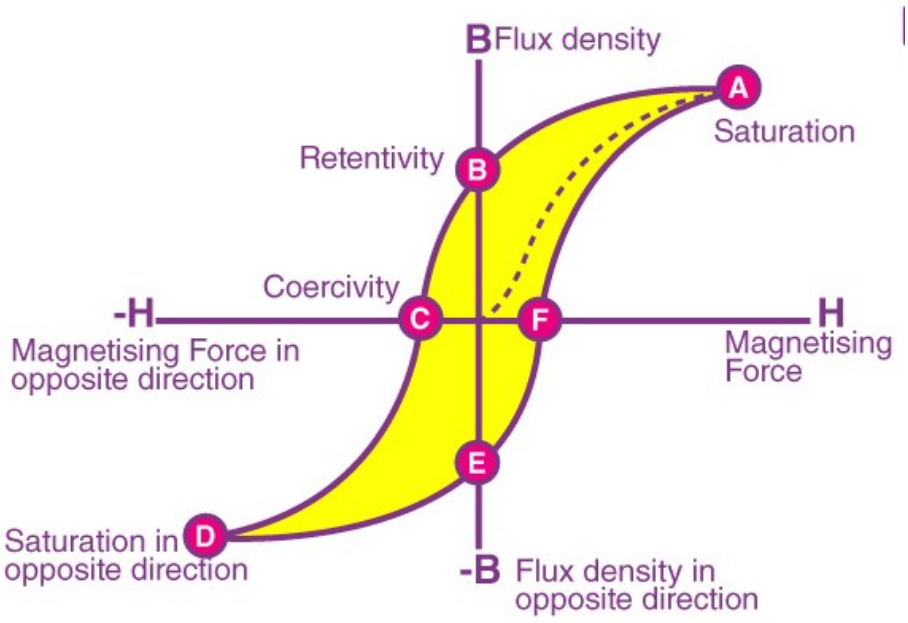

Figure 1.16. Hysteresis loop or B-H curve

The various parameters of the magnetic materials can be determined from the hysteresis loop as given below

(i) Retentivity – It measures a certain amount of residual magnetic field after getting saturation point at magnetizing force (H) is zero. (The value of B at point b on the hysteresis curve.)

Residual Magnetism or **Residual Flux -** The magnetic flux density that remains a material when the magnetizing force is zero. It is remarked that both of retentivity and residual flux density have the same value when the material has been magnetized to the saturation point. It is observed that when the magnetizing force did not attain the saturation level, the level of retentivity may be greater than the value of residual magnetism.

(ii) Coercive Force - The amount of reverse magnetic field that needs to be provided to a magnetic substance for the magnetic flux to return to zero. (On the hysteresis curve, the value of H at point c.)

(iii) Permeability - A material attribute that describes how easily a magnetic flux can be established in a component.

(iv) Reluctance - Reluctance is the resistance of a ferromagnetic material exhibits to the formation of a magnetic field. The resistance in an electrical circuit is equivalent to reluctance.

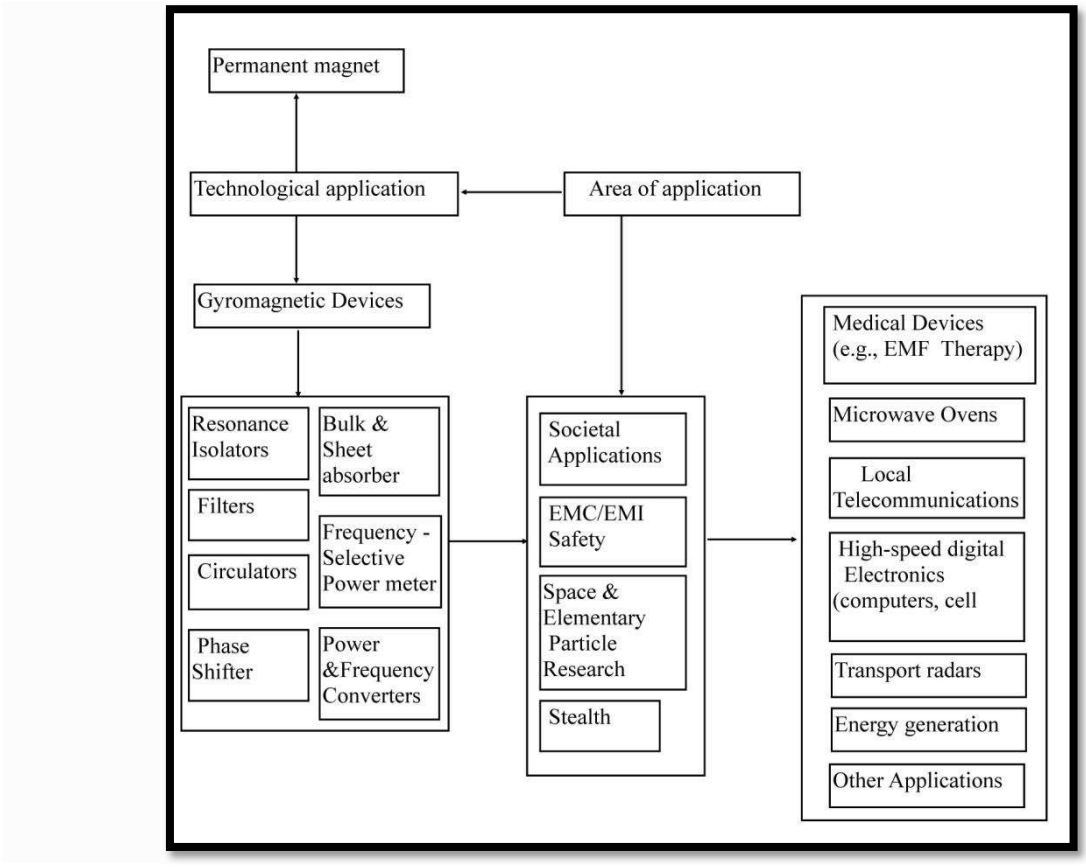

Figure 1.17 Applications of magnetic materials

1.15.4 Aim of the present work

The perovskite material shows simultaneously dielectric and magnetic properties useful in electronic devices such as mobiles, cameras, computers, Television, etc. Scientists are working to develop better electrical devices and memory with a high dielectric constant and low dielectric loss.

(i) The thesis focuses on the synthesis and characterization of ceramic materials, as well as various types of applications such as dielectric and magnetic characteristics.

(ii) Grain and grain boundaries, morphological structure, particle analyzed, temperature and frequency influence on dielectric and electrical characteristics have been investigated extensively.

(iii) To improve the dielectric constant and magnetic properties of ceramic materials that are useful in the field of microelectronic devices and permanent magnets, Semi –the wet and chemical route was to be used to observe and monitor homogeneous mixing of metal ions and material synthesized at low sintering temperature for a shorter time. The objective of the present work is to synthesize the following ceramic material

(i) $CaCu_3Mn_4O_{12}$ synthesized by the chemical route.

(ii) $CaCu_{3-X}Mn_XTi_{4-X}Mn_XO_{12}$ (X=0.1) synthesized by the chemical route.

(iii) $CaCu_3Ti_{4-X}Mn_XO_{12}$ (X=0.1 and 0)

(iV) $CaCu_{3-X}Mn_XTi_4O_{12}$ (X=1,0)synthesized by the semi-wet route

Different types of physiochemical characterization of the following above materials in the sequential steps:

I. X-ray powder diffraction (XRD) study was used for the identification of phase formation and the crystal structure of the materials.

II. Scanning electron microscope (SEM) analysis has been performed for the detailed morphological study of the fractured surface of the materials.

III. Transmission Electron Microscopy (TEM) is useful for particle size determination.

IV. The dielectric properties, dependent on both temperature as well as frequency have been investigated.

V. The magnetic properties of the ceramics studied.

VI. The thermal behavior of the ceramic was studied with the help of Thermogravimetric analysis (TGA).

VII. The oxidation state of the element was to be examined with the help of X-ray Photoelectron Spectroscopy (XPS).

VIII. Metal oxygen bond was to be examined with the help of FT-IR.

IX. Grain and grain boundaries were also studied with the help of Raman spectroscopy.

References

Abe, M., Uchino, K., 1974. X-ray study of the deficient perovskite La23TiO3. *Materials Research Bulletin* **9**, 147–155. https://doi.org/10.1016/0025-5408(74)90194-9

Ahmadipour, M., Ain, M.F., Ahmad, Z.A., 2016. A Short Review on Copper Calcium Titanate (CCTO) Electroceramic: Synthesis, Dielectric Properties, Film Deposition, and Sensing Application. *Nano-Micro Lett.* **8**, 291–311. https://doi.org/10.1007/s40820-016-0089-1

Ali, R., Yashima, M., 2005. Space group and crystal structure of the Perovskite CaTiO3 from 296 to 1720K. *Journal of Solid State Chemistry* **178**, 2867–2872. https://doi.org/10.1016/j.jssc.2005.06.027

Allison, M., 2007. Metrology and analysis of nano-particulate barium titanate dielectric material (Report). Kansas State University.

A. Molina-García, M., V. Rees, N., 2016. Effect of catalyst carbon supports on the oxygen reduction reaction in alkaline media: a comparative study. *RSC Advances* **6**, 94669–94681. https://doi.org/10.1039/C6RA18894J

Amow, G., Au, J., Davidson, I., 2006. Synthesis and characterization of La4Ni3−xCoxO10±δ (0.0≤x≤3.0, Δx=0.2) for solid oxide fuel cell cathodes. *Solid State Ionics*, Solid State Ionics 15: Proceedings of the 15th International Conference on Solid State Ionics, Part I **177**, 1837–1841. https://doi.org/10.1016/j.ssi.2006.01.017

Andres, J., Longo, V., Cavalcante, L., Moreira, M.L., Varela, J., Longo, E., 2012. A fresh look at the structural, ferroelectric and photoluminescent properties in perovskites. *Photoluminescence: Applications, Types and Efficacy* 119–161.

AURIVILLIUS, B., 1949. Mixed Bismuth Oxides with Layer Lattices I. The Structure Type of CaNb_2Bi_2O_9. *Arkiv Kemi* **1**, 463–480.

Awana, V.P.S., Takayama-Muromachi, E., Malik, S.K., Yelon, W.B., Karppinen, M., Yamauchi, H., Krishnamurthy, V.V., 2003. Cation intermixing and ordering phenomenon in M–O layer of MSr2YCu2Oz (M-1212) compounds with M=Fe, Co, Al, and Ga: A neutron powder diffraction study. *Journal of Applied Physics* **93**, 8221–8223. https://doi.org/10.1063/1.1544523

Badr, A.M., Elshaikh, H.A., Ashraf, I.M., 2011. Impacts of Temperature and Frequency on the Dielectric Properties for Insight into the Nature of the Charge Transports in the Tl2S Layered Single Crystals. *Journal of Modern Physics* **2011**. https://doi.org/10.4236/jmp.2011.21004

Bai, Y., Cheng, Z.-Y., Bharti, V., Xu, H.S., Zhang, Q.M., 2000. High-dielectric-constant ceramic-powder polymer composites. *Appl. Phys. Lett.* **76**, 3804–3806. https://doi.org/10.1063/1.126787

Balamurugaraj, P., Suresh, S., Koteeswari, P., Mani, P., 2013. Growth, optical, mechanical, dielectric and photoconductivity properties of L-proline succinate NLO single crystal. *J. Mater. Phys. Chem* **1**, 4–8.

Baltz, V., Manchon, A., Tsoi, M., Moriyama, T., Ono, T., Tserkovnyak, Y., 2018. Antiferromagnetic spintronics. *Rev. Mod. Phys.* **90**, 015005. https://doi.org/10.1103/RevModPhys.90.015005

Banerjee, S., Kim, D.-I., Robinson, R.D., Herman, I.P., Mao, Y., Wong, S.S., 2006. Observation of Fano asymmetry in Raman spectra of SrTiO3 and CaxSr1−xTiO3 perovskite nanocubes. *Appl. Phys. Lett.* **89**, 223130. https://doi.org/10.1063/1.2400095

Bassat, J.-M., Burriel, M., Wahyudi, O., Castaing, R., Ceretti, M., Veber, P., Weill, I., Villesuzanne, A., Grenier, J.-C., Paulus, W., Kilner, J.A., 2013. Anisotropic Oxygen Diffusion Properties in Pr2NiO4+δ and Nd2NiO4+δ Single Crystals. *J. Phys. Chem. C* **117**, 26466–26472. https://doi.org/10.1021/jp409057k

Bibes, M., Barthelemy, A., 2007. Oxide Spintronics. *IEEE Transactions on Electron Devices* **54**, 1003–1023. https://doi.org/10.1109/TED.2007.894366

Bielański, A., Dereń, J., Haber, J., 1957. Electric Conductivity and Catalytic Activity of Semiconducting Oxide Catalysts. *Nature* **179**, 668–669. https://doi.org/10.1038/179668a0

Bochu, B., Deschizeaux, M.N., Joubert, J.C., Collomb, A., Chenavas, J., Marezio, M., 1979. Synthèse et caractérisation d'une série de titanates pérowskites isotypes de [CaCu3](Mn4)O12. *Journal of Solid State Chemistry* **29**, 291–298. https://doi.org/10.1016/0022-4596(79)90235-4

Boonlakhorn, J., Thongbai, P., 2020. Dielectric properties, nonlinear electrical response and microstructural evolution of CaCu3Ti4-xSnxO12 ceramics prepared by a double ball-milling process. *Ceramics International* **46**, 4952–4958. https://doi.org/10.1016/j.ceramint.2019.10.233

Boukenter, A., Champagnon, B., Duval, E., Rousset, J.L., Dumas, J., Serughetti, J., 1988. Vibrational modes in silica aerogels: low-frequency Raman scattering. *J. Phys. C: Solid State Phys.* **21**, L1097–L1102. https://doi.org/10.1088/0022-3719/21/34/001

Boulahya, K., Gil, D.M., Hassan, M., Martin, S.G., Amador, U., 2017. Structural and microstructural characterization and properties of new phases in the Nd–Sr–Co–(Fe/Mn)–O system as air-electrodes in SOFCs. *Dalton Transactions* **46**, 1283–1289. https://doi.org/10.1039/C6DT03970G

Bowers, K.D., Owen, J., 1955. Paramagnetic Resonance II. *Rep. Prog. Phys.* **18**, 304–373. https://doi.org/10.1088/0034-4885/18/1/308

Bueno, P.R., Varela, J.A., Longo, E., 2008. SnO2, ZnO and related polycrystalline compound semiconductors: An overview and review on the voltage-dependent resistance (non-ohmic) feature. *Journal of the European Ceramic Society* **28**, 505–529. https://doi.org/10.1016/j.jeurceramsoc.2007.06.011

Cabuk, S., Akkus, H., Mamedov, A.M., 2007. Electronic and optical properties of KTaO3: Ab initio calculation. *Physica B: Condensed Matter* **394**, 81–85. https://doi.org/10.1016/j.physb.2007.02.012

Cain, M.G., Stewart, M., 2014. Losses in Piezoelectrics via Complex Resonance Analysis. In 'Characterisation of Ferroelectric Bulk Materials and Thin Films' 'Springer Series in Measurement Science and Technology' (Ed. Cain, M.G.). Springer Netherlands, Dordrecht, pp. 233–242. https://doi.org/10.1007/978-1-4020-9311-1_10

Carrasco, J., Illas, F., Lopez, N., Kotomin, E.A., Zhukovskii, Y.F., Evarestov, R.A., Mastrikov, Y.A., Piskunov, S., Maier, J., 2006. First-principles calculations of the atomic and electronic structure of F centers in the bulk and on the (001) surface of Sr Ti O 3. *Physical Review B* **73**, 064106.

Chandler, C.D., Roger, Christophe., Hampden-Smith, M.J., 1993. Chemical aspects of solution routes to perovskite-phase mixed-metal oxides from metal-organic precursors. *Chem. Rev.* **93**, 1205–1241. https://doi.org/10.1021/cr00019a015

Chaudhuri, A., Mandal, K., 2012. Enhancement of ferromagnetic and dielectric properties of lanthanum doped bismuth ferrite nanostructures. *Materials Research Bulletin* **47**, 1057–1061.

Chen, R.R., Sun, Y., Ong, S.J.H., Xi, S., Du, Y., Liu, C., Lev, O., Xu, Z.J., 2020. Antiferromagnetic Inverse Spinel Oxide LiCoVO4 with Spin-Polarized Channels for Water Oxidation. *Advanced Materials* **32**, 1907976. https://doi.org/10.1002/adma.201907976

Chu, L., Li, M., Wan, Z., Ding, L., Song, D., Dou, S., Chen, J., Wang, Y., 2014. Morphology control and fabrication of multi-shelled NiO spheres by tuning the pH value via a hydrothermal process. *CrystEngComm* **16**, 11096–11101.

Cohen, M.H., Neaton, J.B., He, L., Vanderbilt, D., 2003. Extrinsic models for the dielectric response of CaCu3Ti4O12. *Journal of Applied Physics* **94**, 3299–3306. https://doi.org/10.1063/1.1595708

da Conceição, L., Silva, A.M., Ribeiro, N.F.P., Souza, M.M.V.M., 2011. Combustion synthesis of La0.7Sr0.3Co0.5Fe0.5O3 (LSCF) porous materials for application as cathode in IT-SOFC. *Materials Research Bulletin* **46**, 308–314. https://doi.org/10.1016/j.materresbull.2010.10.009

Davies, P.K., Wu, H., Borisevich, A.Y., Molodetsky, I.E., Farber, L., 2008. Crystal chemistry of complex perovskites: new cation-ordered dielectric oxides. *Annu. Rev. Mater. Res.* **38**, 369–401.

Dawber, M., Rabe, K.M., Scott, J.F., 2005. Physics of thin-film ferroelectric oxides. *Reviews of modern physics* **77**, 1083.

De Almeida-Didry, S., Nomel, M.M., Autret, C., Honstettre, C., Lucas, A., Pacreau, F., Gervais, F., 2018. Control of grain boundary in alumina doped CCTO showing colossal permittivity by core-shell approach. *Journal of the European Ceramic Society* **38**, 3182–3187. https://doi.org/10.1016/j.jeurceramsoc.2018.03.003

Demmig-Adams, B., Adams, W.W., 2006. Photoprotection in an ecological context: the remarkable complexity of thermal energy dissipation. *New Phytologist* **172**, 11–21. https://doi.org/10.1111/j.1469-8137.2006.01835.x

Devan, R.S., Deshpande, S.B., Chougule, B.K., 2007. Ferroelectric and ferromagnetic properties of (x) BaTiO3+(1- x) Ni0. 94Co0. 01Cu0. 05 Fe2O4 composite. *Journal of Physics D: Applied Physics* **40**, 1864.

Dion, M., Ganne, M., Tournoux, M., 1981. Nouvelles familles de phases MIMII2Nb3O10 a feuillets “perovskites”. *Materials Research Bulletin* **16**, 1429–1435. https://doi.org/10.1016/0025-5408(81)90063-5

Domen, K., Yoshimura, J., Sekine, T., Tanaka, A., Onishi, T., 1990. A novel series of photocatalysts with an ion-exchangeable layered structure of niobate. *Catalysis letters* **4**, 339–343.

Dubey, A.K., Singh, P., Singh, S., Kumar, D., Parkash, O., 2011. Charge compensation, electrical and dielectric behavior of lanthanum doped CaCu3Ti4O12. *Journal of Alloys and Compounds* **509**, 3899–3906. https://doi.org/10.1016/j.jallcom.2010.12.156

Ebner, C., Stroud, D., 1985. Diamagnetic susceptibility of superconducting clusters: Spin-glass behavior. *Phys. Rev. B* **31**, 165–171. https://doi.org/10.1103/PhysRevB.31.165

Ezhilvalavan, S., Tseng, T.-Y., 2000. Progress in the developments of (Ba,Sr)TiO3 (BST) thin films for Gigabit era DRAMs. *Materials Chemistry and Physics* **65**, 227–248. https://doi.org/10.1016/S0254-0584(00)00253-4

Fang, L., Shen, M., Cao, W., 2004. Effects of postanneal conditions on the dielectric properties of CaCu3Ti4O12 thin films prepared on Pt/Ti/SiO2/Si substrates. *Journal of Applied Physics* **95**, 6483–6485. https://doi.org/10.1063/1.1728308

Fang, P., Fan, H., Xi, Z., Chen, W., 2012. Studies of structural and electrical properties on four-layers Aurivillius phase BaBi4Ti4O15. *Solid State Communications* **152**, 979–983. https://doi.org/10.1016/j.ssc.2012.03.007

Fava, F.F., D\textquotesingleArco, P., Orlando, R., Dovesi, R., 1997. A quantum mechanical investigation of the electronic and magnetic properties of perovskite. *J. Phys.: Condens. Matter* **9**, 489–498. https://doi.org/10.1088/0953-8984/9/2/016

Ferrarelli, M.C., Adams, T.B., Feteira, A., Sinclair, D.C., West, A.R., 2006. High intrinsic permittivity in Na1⁄2Bi1⁄2Cu3Ti4O12. *Appl. Phys. Lett.* **89**, 212904. https://doi.org/10.1063/1.2388251

Galasso, F.S., 2013. Structure, properties and preparation of perovskite-type compounds: international series of monographs in solid state physics. Elsevier.

Garmong, G., Shepard, L.A., 1971. Matrix strengthening mechanisms of an iron fiber-copper matrix composite as a function of fiber size and spacing. *Metall Mater Trans B* **2**, 175–180. https://doi.org/10.1007/BF02662654

Gautam, P., Khare, A., Sharma, S., Singh, N.B., Mandal, K.D., 2016. Characterization of Bi2/3Cu3Ti4O12 ceramics synthesized by semi-wet route. *Progress in Natural Science: Materials International* **26**, 567–571. https://doi.org/10.1016/j.pnsc.2016.11.008

Gautam, P., Yadava, S.S., Khare, A., Mandal, K.D., 2017. Dielectric and magnetic studies of 0.5Bi2/3Cu3Ti4O12 - 0.5Bi3LaTi3O12 nano-composite ceramic synthesized by semi-wet route. *Ceramics International* **43**, 3133–3139. https://doi.org/10.1016/j.ceramint.2016.11.130

Ghorai, S., Ivanov, S.A., Skini, R., Svedlindh, P., 2021. Evolution of Griffiths phase and critical behaviour of La1-x Pb x MnO3$\pm$y solid solutions. *J. Phys.: Condens. Matter* **33**, 145801. https://doi.org/10.1088/1361-648X/abdd64

Goudochnikov, P., Bell, A.J., 2007. Correlations between transition temperature, tolerance factor and cohesive energy in 2$\mathplus$:4$\mathplus$ perovskites. *J. Phys.: Condens. Matter* **19**, 176201. https://doi.org/10.1088/0953-8984/19/17/176201

Hamid, A.S., Uedono, A., Chikyow, T., Uwe, K., Mochizuki, K., Kawaminami, S., 2006. Vacancy-type defects and electronic structure of perovskite-oxide SrTiO3 from positron annihilation. *physica status solidi (a)* **203**, 300–305. https://doi.org/10.1002/pssa.200521209

Hao, W., Zhang, J., Tan, Y., Su, W., 2009. Giant Dielectric-Permittivity Phenomena of Compositionally and Structurally CaCu3Ti4O12-Like Oxide Ceramics. *Journal of the American Ceramic Society* **92**, 2937–2943. https://doi.org/10.1111/j.1551-2916.2009.03298.x

Hardy, A., Mondelaers, D., Van Bael, M.K., Mullens, J., Van Poucke, L.C., Vanhoyland, G., D'Haen, J., 2004. Synthesis of (Bi,La)4Ti3O12 by a new aqueous solution-gel route. *Journal of the European Ceramic Society*, Electroceramics VIII **24**, 905–909. https://doi.org/10.1016/S0955-2219(03)00420-5

He, J., Borisevich, A., Kalinin, S.V., Pennycook, S.J., Pantelides, S.T., 2010. Control of Octahedral Tilts and Magnetic Properties of Perovskite Oxide Heterostructures by Substrate Symmetry. *Phys. Rev. Lett.* **105**, 227203. https://doi.org/10.1103/PhysRevLett.105.227203

Heiland, G., 1954. Zum Einfluß von adsorbiertem Sauerstoff auf die elektrische Leitfähigkeit von Zinkoxydkristallen. *Zeitschrift für Physik* **138**, 459–464.

Holtzworth-Munroe, A., Jacobson, N.S., 1985. Causal attributions of married couples: When do they search for causes? What do they conclude when they do? *Journal of Personality and Social Psychology* **48**, 1398–1412. https://doi.org/10.1037/0022-3514.48.6.1398

Homes, C.C., Vogt, T., Shapiro, S.M., Wakimoto, S., Ramirez, A.P., 2001. Optical Response of High-Dielectric-Constant Perovskite-Related Oxide. *Science* **293**, 673–676. https://doi.org/10.1126/science.1061655

Hu, G.D., Cheng, X., Wu, W.B., Yang, C.H., 2007. Effects of Gd substitution on structure and ferroelectric properties of BiFeO3 thin films prepared using metal organic decomposition. *Appl. Phys. Lett.* **91**, 232909. https://doi.org/10.1063/1.2822826

Huijben, M., Rijnders, G., Blank, D.H.A., Bals, S., Aert, S.V., Verbeeck, J., Tendeloo, G.V., Brinkman, A., Hilgenkamp, H., 2006. Electronically coupled complementary interfaces between perovskite band insulators. *Nature Mater* **5**, 556–560. https://doi.org/10.1038/nmat1675

Huízar-Félix, A.M., Hernández, T., de la Parra, S., Ibarra, J., Kharisov, B., 2012. Sol–gel based Pechini method synthesis and characterization of Sm1−xCaxFeO3 perovskite 0.1≤x≤0.5. *Powder Technology* **229**, 290–293. https://doi.org/10.1016/j.powtec.2012.06.057

Jacobson, A.J., Johnson, J.W., Lewandowski, J.T., 2002. Interlayer chemistry between thick transition-metal oxide layers: synthesis and intercalation reactions of K[Ca2Nan-3NbnO3n+1] (3 .ltoreq. n .ltoreq. 7) [WWW Document]. *ACS Publications*. https://doi.org/10.1021/ic00217a006

Jang, Y.-I., Moorehead, W.D., Chiang, Y.-M., 2002. Synthesis of the monoclinic and orthorhombic phases of LiMnO2 in oxidizing atmosphere. *Solid State Ionics* **149**, 201–207. https://doi.org/10.1016/S0167-2738(02)00176-5

Joanni, E., Savu, R., Bueno, P.R., Longo, E., Varela, J.A., 2008. P-type semiconducting gas sensing behavior of nanoporous rf sputtered CaCu3Ti4O12 thin films. *Appl. Phys. Lett.* **92**, 132110. https://doi.org/10.1063/1.2905810

Jonker, G.H., 1954. Semiconducting properties of mixed crystals with perovskite structure. *Physica* **20**, 1118–1122. https://doi.org/10.1016/S0031-8914(54)80250-3

Kato, S., Ogasawara, M., Sugai, M., Nakata, S., 2004. Crystal Structure and Property of Perovskite-Type Oxides Containing Ion Vacancy. *Catalysis Surveys from Asia* **8**, 27–34. https://doi.org/10.1023/B:CATS.0000015112.82947.8e

Kawasaki, S., Takano, M., Takeda, Y., 1996. Ferromagnetic Properties of SrFe1−xCoxO3Synthesized under High Pressure. *Journal of Solid State Chemistry* **121**, 174–180. https://doi.org/10.1006/jssc.1996.0025

Kestigian, M., Dickinson, J.G., Ward, R., 1957. Ion-deficient phases in titanium and vanadium compounds of the perovskite type1, 2. *Journal of the American Chemical Society* **79**, 5598–5601.

Kharton, V.V., Viskup, A.P., Kovalevsky, A.V., Naumovich, E.N., Marques, F.M.B., 2001. Ionic transport in oxygen-hyperstoichiometric phases with K2NiF4-type structure. *Solid State Ionics* **143**, 337–353. https://doi.org/10.1016/S0167-2738(01)00876-1

Khenata, R., Sahnoun, M., Baltache, H., Rérat, M., Rashek, A.H., Illes, N., Bouhafs, B., 2005. First-principle calculations of structural, electronic and optical properties of BaTiO3 and BaZrO3 under hydrostatic pressure. *Solid State Communications* **136**, 120–125. https://doi.org/10.1016/j.ssc.2005.04.004

Kim, I.-D., Rothschild, A., Hyodo, T., Tuller, H.L., 2006. Microsphere templating as means of enhancing surface activity and gas sensitivity of CaCu3Ti4O12 thin films. *Nano letters* **6**, 193–198.

Kim, J., Yin, X., Tsao, K.-C., Fang, S., Yang, H., 2014. Ca2Mn2O5 as Oxygen-Deficient Perovskite Electrocatalyst for Oxygen Evolution Reaction. *J. Am. Chem. Soc.* **136**, 14646–14649. https://doi.org/10.1021/ja506254g

Koehler, W.C., Wollan, E.O., 1957. Neutron-diffraction study of the magnetic properties of perovskite-like compounds LaBO3. *Journal of Physics and Chemistry of Solids* **2**, 100–106. https://doi.org/10.1016/0022-3697(57)90095-1

Koops, C.G., 1951. On the Dispersion of Resistivity and Dielectric Constant of Some Semiconductors at Audiofrequencies. *Phys. Rev.* **83**, 121–124. https://doi.org/10.1103/PhysRev.83.121

Kretly, L.C., Almeida, A.F.L., Oliveira, R.S. de, Sasaki, J.M., Sombra, A.S.B., 2003. Electrical and optical properties of CaCu3Ti4O12 (CCTO) substrates for microwave devices and antennas. *Microwave and Optical Technology Letters* **39**, 145–150. https://doi.org/10.1002/mop.11152

Kuczenski, R., Segal, D., 1989. Concomitant characterization of behavioral and striatal neurotransmitter response to amphetamine using in vivo microdialysis. *J. Neurosci.* **9**, 2051–2065.

Kumar, A., Verma, M.K., Singh, S., Das, T., Singh, L., Mandal, K.D., 2020a. Electrical, Magnetic and Dielectric Properties of Cobalt-Doped Barium Hexaferrite BaFe12−xCoxO19 (x = 0.0, 0.05, 0.1 and 0.2) Ceramic Prepared via a Chemical Route. *Journal of Elec Materi* **49**, 6436–6447. https://doi.org/10.1007/s11664-020-08364-8

Kumar, B.R., Rao, T.S., 2012. AFM studies on surface morphology, topography and texture of nanostructured zinc aluminum oxide thin films. *Digest Journal of Nanomaterials and Biostructures* **7**, 1881–1889.

Kumar, L., Mohanty, P., Shripathi, T., Rath, C., 2009. Appearance of superparamagnetic phase below Curie temperature in cobalt chromite nanoparticles. *Nanoscience and Nanotechnology Letters* **1**, 199–203.

Kumar, V., Kumar, A., Verma, M.K., Singh, S., Pandey, S., Rai, V.S., Prajapati, D., Das, T., Singh, N.B., Mandal, K.D., 2020b. Investigation of dielectric and electrochemical behavior of CaCu3−xMnxTi4O12 (x = 0, 1) ceramic synthesized through semi-wet route. *Materials Chemistry and Physics* **245**, 122804. https://doi.org/10.1016/j.matchemphys.2020.122804

Kumar, V., Kumar, A., Verma, M.K., Singh, S., Pandey, S., Singh, L., Singh, N.B., Mandal, K.D., 2020c. Observation of unusual Griffith's phase behavior in quadruple perovskite oxide CaCu3Mn4O12 (CCMO) synthesized through chemical route. *Arabian Journal of Chemistry* **13**, 4895–4903. https://doi.org/10.1016/j.arabjc.2020.01.003

Kuo, D.-H., Chang, C.-C., Su, T.-Y., Wang, W.-K., Lin, B.-Y., 2001. Dielectric behaviours of multi-doped BaTiO3/epoxy composites. *Journal of the European Ceramic Society* **21**, 1171–1177. https://doi.org/10.1016/S0955-2219(00)00327-7

Lawn, J.E., Blencowe, H., Waiswa, P., Amouzou, A., Mathers, C., Hogan, D., Flenady, V., Frøen, J.F., Qureshi, Z.U., Calderwood, C., Shiekh, S., Jassir, F.B., You, D., McClure, E.M., Mathai, M., Cousens, S., Flenady, V., Frøen, J.F., Kinney, M.V., de Bernis, L., Lawn, J.E., Blencowe, H., Heazell, A., Leisher, S.H., Azad, K., Rahman, A., El-Arifeen, S., Day, L.T., Shah, S.L., Alam, S., Wangdi, S., Ilboudo, T.F., Zhu, J., Liang, J., Mu, Y., Li, X., Zhong, N., Kyprianou, T., Allvee, K.,

Gissler, M., Zeitlin, J., Bah, A., Jawara, L., Waiswa, P., Lack, N., de Maria Herandez, F., Shah More, N., Nair, N., Tripathy, P., Kumar, R., Newtonraj, A., Kaur, M., Gupta, M., Varghese, B., Isakova, J., Phiri, T., Hall, J.A., Curteanu, A., Manandhar, D., Hukkelhoven, C., Dijs-Elsinga, J., Klungsøyr, K., Poppe, O., Barros, H., Correia, S., Tsiklauri, S., Cap, J., Podmanicka, Z., Szamotulska, K., Pattison, R., Hassan, A.A., Musafi, A., Kujala, S., Bergstrom, A., Langhoff -Roos, J., Lundqvist, E., Kadobera, D., Costello, A., Colbourn, T., Fottrell, E., Prost, A., Osrin, D., King, C., Neuman, M., Hirst, J., Rubayet, S., Smith, L., Manktelow, B.N., Draper, E.S., 2016. Stillbirths: rates, risk factors, and acceleration towards 2030. *The Lancet* **387**, 587–603. https://doi.org/10.1016/S0140-6736(15)00837-5

Lee, H.N., Visinoiu, A., Senz, S., Harnagea, C., Pignolet, A., Hesse, D., Gösele, U., 2000. Structural and electrical anisotropy of (001)-, (116)-, and (103)-oriented epitaxial SrBi2Ta2O9 thin films on SrTiO3 substrates grown by pulsed laser deposition. *Journal of Applied Physics* **88**, 6658–6664. https://doi.org/10.1063/1.1321776

Lettieri, J., Zurbuchen, M.A., Jia, Y., Schlom, D.G., Streiffer, S.K., Hawley, M.E., 2000. Epitaxial growth of non-c-oriented SrBi2Nb2O9 on (111) SrTiO3. *Appl. Phys. Lett.* **76**, 2937–2939. https://doi.org/10.1063/1.126522

Li, J.Y., Zhao, X.T., Li, S.T., Alim, M.A., 2010. Intrinsic and extrinsic relaxation of CaCu3Ti4O12 ceramics: Effect of sintering. *Journal of Applied Physics* **108**, 104104. https://doi.org/10.1063/1.3511444

Liu, L., Gao, J., Liu, P., Duan, X., Han, N., Li, F., Sofianos, M.V., Wang, S., Tan, X., Liu, S., 2019. Novel applications of perovskite oxide via catalytic peroxymonosulfate advanced oxidation in aqueous systems for trace L-cysteine detection. *Journal of Colloid and Interface Science* **545**, 311–316. https://doi.org/10.1016/j.jcis.2019.03.045

Maaz, K., Mumtaz, A., Hasanain, S.K., Bertino, M.F., 2010. Temperature dependent coercivity and magnetization of nickel ferrite nanoparticles. *Journal of Magnetism and Magnetic Materials* **322**, 2199–2202. https://doi.org/10.1016/j.jmmm.2010.02.010

Mannath, D., Schaper, L.W., Ulrich, R.K., 2004. Advanced decoupling in high performance IC packaging. In '2004 Proceedings. 54th Electronic Components and Technology Conference (IEEE Cat. No.04CH37546)'. Presented at the 2004 Proceedings. 54th Electronic Components and Technology Conference (IEEE Cat. No.04CH37546), pp. 266-270 Vol.1. https://doi.org/10.1109/ECTC.2004.1319349

Markovich, V., Wisniewski, A., Szymczak, H., 2014. Chapter One - Magnetic Properties of Perovskite Manganites and Their Modifications. In 'Handbook of Magnetic Materials' (Ed. Buschow, K.H.J.). Elsevier, pp. 1–201. https://doi.org/10.1016/B978-0-444-63291-3.00001-5

Nair, H., Swain, D., Nhalil, H., Adiga, S., Narayana, C., Elizabeth, S., 2011. Griffiths phase-like behavior and spin-phonon coupling in double perovskite Tb2NiMnO6. *Journal of Applied Physics* **110**, 123919. https://doi.org/10.1063/1.3671674

Pathania, D., Millard, M., Neamati, N., 2009. Opportunities in discovery and delivery of anticancer drugs targeting mitochondria and cancer cell metabolism. *Advanced Drug Delivery*

Reviews, Mitochondrial Medicine and Therapeutics, Part II **61**, 1250–1275. https://doi.org/10.1016/j.addr.2009.05.010

Rajeswari, M., Shreekala, R., Goyal, A., Lofland, S.E., Bhagat, S.M., Ghosh, K., Sharma, R.P., Greene, R.L., Ramesh, R., Venkatesan, T., Boettcher, T., 1998. Correlation between magnetic homogeneity, oxygen content, and electrical and magnetic properties of perovskite manganite thin films. *Appl. Phys. Lett.* **73**, 2672–2674. https://doi.org/10.1063/1.122549

Reed, M.L., El-Masry, N.A., Stadelmaier, H.H., Ritums, M.K., Reed, M.J., Parker, C.A., Roberts, J.C., Bedair, S.M., 2001. Room temperature ferromagnetic properties of (Ga, Mn)N. *Appl. Phys. Lett.* **79**, 3473–3475. https://doi.org/10.1063/1.1419231

Richerson, D.W., Lee, W.E., 1992. Modern Ceramic Engineering: Properties, Processing, and Use in Design, Third Edition. CRC Press.

Rossouw, J.E., Prentice, R.L., Manson, J.E., Wu, L., Barad, D., Barnabei, V.M., Ko, M., LaCroix, A.Z., Margolis, K.L., Stefanick, M.L., 2007. Postmenopausal Hormone Therapy and Risk of Cardiovascular Disease by Age and Years Since Menopause. *JAMA* **297**, 1465–1477. https://doi.org/10.1001/jama.297.13.1465

Roy, S., Dubenko, I.S., Khan, M., Condon, E.M., Craig, J., Ali, N., Liu, W., Mitchell, B.S., 2005. Magnetic properties of perovskite-derived air-synthesized $R\mathrm{Ba}{\mathrm{Co}}_{2}{\mathrm{O}}_{5+\ensuremath{\delta}}$ $(R=\mathrm{La}\mathrm{Ho})$ compounds. *Phys. Rev. B* **71**, 024419. https://doi.org/10.1103/PhysRevB.71.024419

Salame, P., Drai, R., Prakash, O., Kulkarni, A.R., 2014. IBLC effect leading to colossal dielectric constant in layered structured Eu2CuO4 ceramic. *Ceramics International* **40**, 4491–4498. https://doi.org/10.1016/j.ceramint.2013.08.123

Sapozhnik, A.A., Abrudan, R., Skourski, Y., Jourdan, M., Zabel, H., Kläui, M., Elmers, H.-J., 2017. Manipulation of antiferromagnetic domain distribution in Mn2Au by ultrahigh magnetic fields and by strain. *physica status solidi (RRL) – Rapid Research Letters* **11**, 1600438. https://doi.org/10.1002/pssr.201600438

Satyanarayana, K.G., Sukumaran, K., Mukherjee, P.S., Pavithran, C., Pillai, S.G.K., 1990. Natural fibre-polymer composites. *Cement and Concrete Composites* **12**, 117–136. https://doi.org/10.1016/0958-9465(90)90049-4

Shamonina, E., Solymar, L., 2004. Diamagnetic properties of metamaterials: a magnetostatic analogy. *Eur. Phys. J. B* **41**, 307–312. https://doi.org/10.1140/epjb/e2004-00322-7

Sharma, S., M. Singh, M., D. Mandal, K., 2018. Microstructure, crystal structure modelling and dielectric properties of Y 2/3 Cu 3−x Zn x Ti 4 O 12 (x = 0.10, 0.20 and 0.30) ceramics. *New Journal of Chemistry* **42**, 14655–14667. https://doi.org/10.1039/C8NJ02105H

Sharma, S., Yadav, S.S., Singh, M.M., Mandal, K.D., 2014. Impedance spectroscopic and dielectric properties of nanosized Y2/3Cu3Ti4O12 ceramic. *J. Adv. Dielect.* **04**, 1450030. https://doi.org/10.1142/S2010135X14500301

Shimakawa, Y., 2015. Crystal and magnetic structures of CaCu3Fe4O12and LaCu3Fe4O12: distinct charge transitions of unusual high valence Fe. *J. Phys. D: Appl. Phys.* **48**, 504006. https://doi.org/10.1088/0022-3727/48/50/504006

Singh, L., Rai, U.S., Mandal, K.D., 2013. Dielectric properties of zinc doped nanocrystalline calcium copper titanate synthesized by different approach. *Materials Research Bulletin* **48**, 2117–2122. https://doi.org/10.1016/j.materresbull.2013.02.005

Smith, M.B., Page, K., Siegrist, T., Redmond, P.L., Walter, E.C., Seshadri, R., Brus, L.E., Steigerwald, M.L., 2008. Crystal Structure and the Paraelectric-to-Ferroelectric Phase Transition of Nanoscale BaTiO3. *J. Am. Chem. Soc.* **130**, 6955–6963. https://doi.org/10.1021/ja0758436

Tripathy, N., Das, K.C., Ghosh, S.P., Bose, G., Kar, J.P., 2016. Fabrication of high-k dielectric Calcium Copper Titanate (CCTO) target by solid state route. *IOP Conf. Ser.: Mater. Sci. Eng.* **115**, 012022. https://doi.org/10.1088/1757-899X/115/1/012022

Usov, N.A., Rytov, R.A., Bautin, V.A., 2021. Properties of assembly of superparamagnetic nanoparticles in viscous liquid. *Sci Rep* **11**, 6999. https://doi.org/10.1038/s41598-021-86323-x

Yadava, S.S., Khare, A., Gautam, P., Kumar, A., Mandal, K.D., 2017. Dielectric, ferroelectric and magnetic study of iron doped hexagonal Ba4YMn3O11.5−δ (BYMO) and its dependence on temperature as well as frequency. *New J. Chem.* **41**, 4611–4617. https://doi.org/10.1039/C6NJ04071C

Yadava, S.S., Khare, A., Gautam, P., Singh, L., Lee, Y., Mandal, K.D., 2016. Dielectric, ferroelectric and magnetic properties of hexagonal Ba6Y2Ti4O17 (BYTO) perovskite derived from semi wet route. *RSC Adv.* **6**, 104941–104948. https://doi.org/10.1039/C6RA23418F

Yang, S., Zhang, H., Zhang, S.-W., Zhang, B.-P., 2011. Electrical properties tailoring in Ni-particle-dispersed (Ba0.95Ca0.05)(Ti0.96Zr0.04)O3 composites. *Materials Chemistry and Physics* **126**, 729–733. https://doi.org/10.1016/j.matchemphys.2010.12.052

Yu, L.-M., Zhu, Y.-C., Liu, Y.-L., Qu, P., Xu, M.-T., Shen, Q., Zhao, W.-W., 2018. Ferroelectric Perovskite Oxide@TiO2 Nanorod Heterostructures: Preparation, Characterization, and Application as a Platform for Photoelectrochemical Bioanalysis. *Anal. Chem.* **90**, 10803–10811. https://doi.org/10.1021/acs.analchem.8b01820

Zhao, M.-H., Wang, Z.-L., Mao, S.X., 2004. Piezoelectric Characterization of Individual Zinc Oxide Nanobelt Probed by Piezoresponse Force Microscope. *Nano Lett.* **4**, 587–590. https://doi.org/10.1021/nl035198a

Zhuk, N.A., Shugurov, S.M., Belyy, V.A., Makeev, B.A., Yermolina, M.V., Beznosikov, D.S., Koksharova, L.A., 2018. Thermal stability of CaCu3Ti4O12: Simultaneous thermal analysis and high-temperature mass spectrometric study. *Ceramics International* **44**, 20841–20844.